logical findings and tumorigenesis in GCs. However, the clinical importance of intestinal mucin in GCs is still controversial and no definite conclusions have been reached [12–18]. Candidate genes controlling gastric and intestinal phenotypes include several transcription factors [19]. The caudal-related homeobox 2 gene (CDX2) is an intestine-specific transcription factor that is expressed in nonneoplastic mucosa from the duodenum to the distal colon and is detected in GC with the intestinal phenotype [20]. SOX2, an Sry-like high-mobility group box gastric transcription factor, is expressed in normal gastric mucosa and GC with the gastric phenotype [21]. By performing microarray analyses, we recently discovered that the expression of connexin 30 was observed in intestinal phenotype GC.

Connexins, a family of 20 transmembrane proteins in humans, comprise the main subunits of gap junctions, which are specialized clusters of intercellular channels that allow adjacent cells to directly share ions and hydrophilic molecules of up to 1 kDa in size [22]. Gap junctional intercellular communication (GJIC) is thought to control tissue homeostasis and to coordinate cellular processes such as proliferation, migration, and differentiation [23, 24]. Neoplastic transformation is frequently associated with a loss of GJIC and with a reduced expression of connexins in various tumors [25, 26]. The forced expression of connexins in connexin-deficient cell lines results in the inhibition of tumor growth and the induction of apoptosis in vitro as well as the prevention of tumor formation in vivo [27, 28]. On the other hand, accumulating evidence indicates that connexin 26, a connexin family member, is overexpressed in carcinomas including those of the head and neck, colon, and pancreas [29–32]. Increased connexin 26 expression has been observed in invasive breast carcinomas and metastatic lymph nodes [33, 34]. Together, these strands of evidence appear to contradict the conventionally held view of the role of connexins as tumor suppressors. The localization of connexin 30 has been observed in normal skin [35], cochlea [36] and brain [37]. Connexin 30 gene mutations cause dominant nonsyndromic hearing loss [38, 39], and they have been identified in Clouston syndrome (hidrotic ectodermal dysplasia) [40]. Little is known about the role of connexin 30 in human neoplasia. While the expression of connexin 30 is decreased in human head and neck cancer [41] and in cervical dysplasia of the uterus [42], connexin 30 is upregulated in human skin tumors [43]. Thus, the exact pathogenic mechanisms associated with connexin 30 in carcinogenesis remain obscure.

The present study represents the first detailed analysis of connexin 30 expression in GC. To clarify the pattern of expression and localization of connexin 30 in GC, we performed immunohistochemical analysis of surgically resected GC samples. In addition, we investigated the association between connexin 30 and various markers determining the gastric/intestinal phenotypes (MUC5AC, MUC6, MUC2, and CD10).

Materials and Methods

Tissue Samples

Primary tumor samples and the corresponding nonneoplastic gastric mucosa were collected from 169 patients with GC (123 men and 46 women; age range 29–88 years; mean 70 years). Patients were treated at Hiroshima University Hospital or affiliated hospitals. For RNA extraction, tissue samples obtained at the time of surgery were immediately embedded in OCT compound (Sakura Finetechnical Co., Ltd., Tokyo, Japan), frozen in liquid nitrogen, and stored at −80°C. For quantitative reverse transcription-polymerase chain reaction (RT-PCR) analysis, 18 GC samples and the corresponding nonneoplastic mucosa samples were used. The samples were obtained during surgery at Hiroshima University Hospital. We confirmed microscopically that the tumor specimens were predominantly (>50%) cancer tissue. Samples were frozen immediately in liquid nitrogen and stored at −80°C until used. Samples of normal brain, spinal cord, heart, skeletal muscle, lung, stomach, small intestine, colon, liver, pancreas, kidney, uterus, bone marrow, spleen, peripheral leukocytes, and trachea were purchased from Clontech (Palo Alto, Calif., USA). For immunohistochemical analysis we used archival formalin-fixed paraffin-embedded tissues from 169 patients who had undergone surgical excision for GC. The 169 GC cases were histologically classified as 102 of the differentiated type and 67 of the undifferentiated type, according to the Japanese Classification of Gastric Carcinomas [44]. Tumor staging was carried out according to the TNM classification [45]. Because written informed consent was not obtained, identifying information for all samples was removed before analysis for strict privacy protection. This procedure was in accordance with the Ethical Guidelines for Human Genome/Gene Research enacted by the Japanese government.

Quantitative RT-PCR

Total RNA was extracted with an RNeasy Mini Kit (Qiagen, Valencia, Calif., USA), and 1 μg of total RNA was converted to cDNA with a First Strand cDNA Synthesis Kit (Amersham Biosciences, Piscataway, N.J., USA). Quantitation of *Connexin 30* mRNA levels in human tissue samples was done by real-time fluorescence detection as described previously [46]. *Connexin 30* primer sequences were 5′-CAG TTG CCT TCT CTC CGA GG-3′ and 5′-CAT GGG ATG TTA CAC ACG CC-3′. PCR was performed with a SYBR Green PCR Core Reagents Kit (Applied Biosystems, Foster City, Calif., USA). Real-time detection of the emission intensity of SYBR Green bound to double-stranded DNA was performed with an ABI PRISM 7700 Sequence Detection System (Applied Biosystems) as described previously [47]. *ACTB*-specific

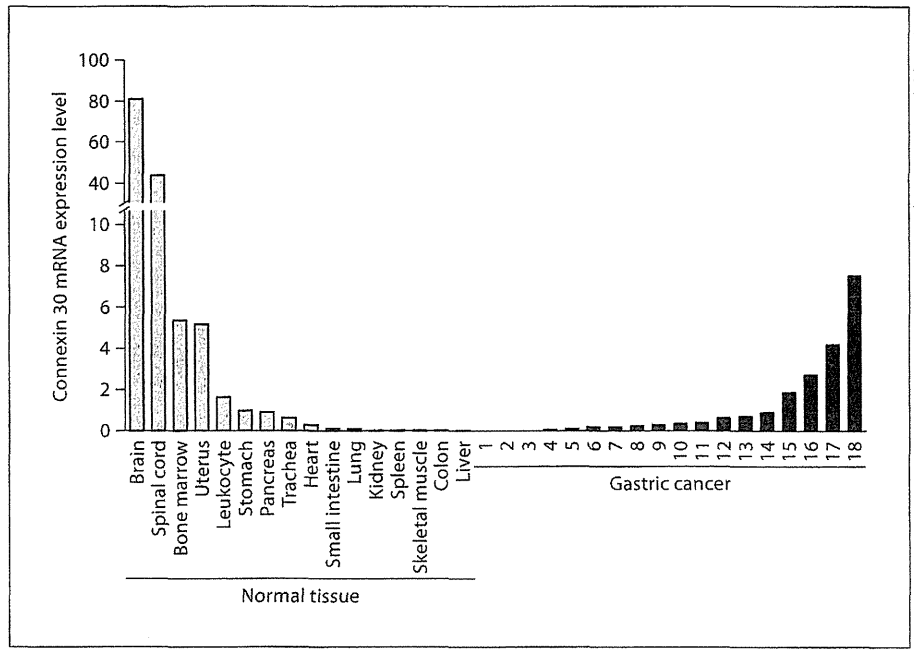

Fig. 1. Quantitative RT-PCR analysis of *connexin 30* in various human normal tissues and GC tissues. Clear *connexin 30* expression is present in normal brain, spinal cord, bone marrow, uterus, etc. High levels of *connexin 30* were observed in some GCs. The units are arbitrary and *connexin 30* expression was calculated by the standardization of 1.0 μg of total RNA from normal stomach as 1.0.

PCR products were amplified from the same RNA samples and served as internal controls.

Antibodies

Anti-connexin 30 antibody was purchased from Invitrogen/Zymed Laboratories, Inc. (San Francisco, Calif., USA). We used 4 antibodies for analysis of the GC phenotypes: anti-MUC5AC (Novocastra, Newcastle, UK) as a marker of gastric foveolar epithelial cells, anti-MUC6 (Novocastra) as a marker of pyloric gland cells, anti-MUC2 (Novocastra) as a marker of goblet cells in the small intestine and colorectum, and anti-CD10 (Novocastra) as a marker of microvilli of absorptive cells in the small intestine and colorectum.

Immunohistochemistry

A Dako LSAB Kit (Dako, Carpinteria, Calif., USA) was used for immunohistochemical analysis. In brief, sections were pretreated by microwave treatment in citrate buffer for 15 min to retrieve antigenicity. After peroxidase activity was blocked with 3% H_2O_2-methanol for 10 min, sections were incubated with normal goat serum (Dako) for 20 min to block nonspecific antibody binding sites. Sections were incubated with the following primary antibodies: anti-connexin 30, anti-MUC5AC, anti-MUC6, anti-MUC2, and anti-CD10 (all diluted 1:50). Sections were incubated with primary antibody for 1 h at 25°C, followed by incubations with biotinylated mouse anti-rabbit IgG and peroxidase-labeled streptavidin for 10 min each. Staining was completed with a 10-min incubation with the substrate-chromogen solution. The sections were counterstained with 0.1% hematoxylin.

Connexin 30 staining was classified according to the percentage of stained cancer cells. Expression was considered to be 'negative' if <10% of cancer cells were stained. When at least 10% of cancer cells were stained, the result of immunostaining was considered 'positive'.

GC cases were classified into 4 phenotypes: gastric phenotype, intestinal phenotype, gastric and intestinal mixed phenotype, and unclassified phenotype. The criteria [20] for the classification of gastric phenotype and intestinal phenotype were as follows: GCs in which more than 10% of the cells displayed the gastric or intestinal epithelial cell phenotype were gastric phenotype or intestinal phenotype cancers, respectively; those sections that showed both gastric and intestinal phenotypes were classified as gastric and intestinal mixed phenotype, and those that lacked both the gastric and the intestinal phenotypes were classified as the unclassified phenotype.

Double Immunofluorescence Staining

Double immunofluorescence staining was performed as described previously [48]. Alexa Fluor 488-conjugated chicken anti-rabbit IgG and Alexa Fluor 546-conjugated goat anti-mouse IgG were used as secondary antibodies (Molecular Probes, Eugene, Oreg., USA).

Statistical Methods

Correlations between clinicopathologic parameters and connexin 30 staining were analyzed by Fisher's exact test. $p < 0.05$ was considered statistically significant.

Results

Expression of Connexin 30 *in Systemic Normal Tissues and GC Tissues*

Quantitative RT-PCR was performed to investigate the specificity of *connexin 30* expression in 16 normal organs. As shown in figure 1, *connexin 30* expression was clearly

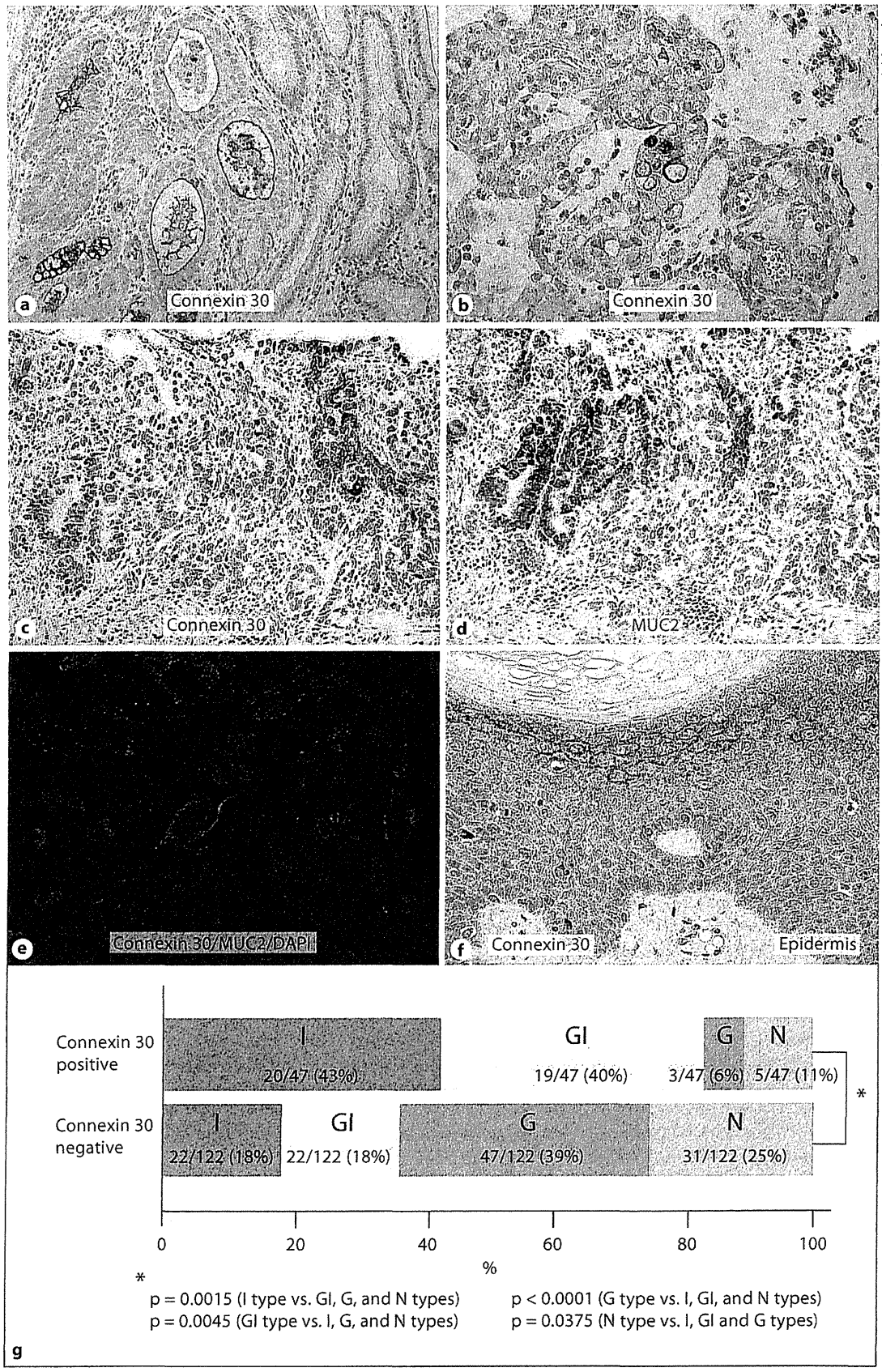
Color version available online
a
Connexin 30
b
Connexin 30
c
Connexin 30
d
MUC2
e
Connexin 30/MUC2/DAPI
f
Connexin 30
Epidermis
g
Connexin 30 positive
I
20/47 (43%)
GI
19/47 (40%)
G
N
3/47 (6%)
5/47 (11%)
*
Connexin 30 negative
I
22/122 (18%)
GI
22/122 (18%)
G
47/122 (39%)
N
31/122 (25%)
0
20
40
60
80
100
%
*
p = 0.0015 (I type vs. GI, G, and N types)
p = 0.0045 (GI type vs. I, G, and N types)
p < 0.0001 (G type vs. I, GI, and N types)
p = 0.0375 (N type vs. I, GI and G types)

Table 1. Relationship between connexin 30 expression and clinicopathologic parameters in 169 GC cases

	Connexin 30 expression		p value
	positive (n = 47)	negative (n = 122)	
Age			
≤65 years (n = 46)	13 (28)	33	NS
>65 years (n = 123)	34 (28)	89	
Gender			
Male (n = 123)	33 (27)	90	NS
Female (n = 46)	14 (30)	32	
Histology[1]			
Differentiated (n = 102)	41 (40)	61	<0.0001
Undifferentiated (n = 67)	6 (9)	61	
T grade			
T1 (n = 83)	35 (42)	48	<0.0001
T2/T3/T4 (n = 86)	12 (14)	74	
N grade			
N0 (n = 107)	37 (35)	70	0.0123
N1/N2/N3 (n = 62)	10 (16)	52	
M grade			
M0 (n = 163)	47 (29)	116	NS
M1 (n = 6)	0 (0)	6	
Stage[2]			
Stage 0/I (n = 104)	38 (37)	66	0.0014
Stage II/III/IV (n = 65)	9 (14)	56	

Figures in parentheses are percentages. p values were calculated by Fisher's exact test. NS = Not significant.

[1] Histology was classified according to the Japanese Classification of Gastric Carcinomas.

[2] Tumor stage was classified according to International Union Against Cancer TNM classification of malignant tumors criteria.

Fig. 2. Immunohistochemical staining of connexin 30 and MUC2 in GC tissues (**a–e**). Connexin 30 was detected in the apical membranes of both well-differentiated GC (**a**) and poorly differentiated GC (**b**), but not in noncancerous epithelium. Serial sections showed that expression of connexin 30 (**c**) was partly adjacent to cytoplasmic expression of MUC2 (**d**). Double-immunostaining of connexin 30 (red) and MUC2 (green) revealed no colocalization of both molecules (**e**). Nuclei are stained with 4′,6-diamidino-2-phenylindole (DAPI; blue). Immunostaining of human epidermis as a positive control showed that connexin 30 was distributed in the keratinocytes of the upper spinous layers and the granular layers (**f**). Summary of connexin 30 expression and expression of the GC mucin phenotype (**g**). Expression of connexin 30 was observed more frequently in I-type and GI-type GC than in other (G and N) GC types. p values were statistically analyzed by Fisher's exact test. Colors refer to the online version only.

detected in the brain and the spinal cord and to a lesser extent in the bone marrow and uterus. However, the expression of *connexin 30* was detected at low levels, or not at all, in other normal organs including the stomach. These results are consistent with those of a previous report [37]. Next, we analyzed quantitative RT-PCR in 18 GC samples. High levels of *connexin 30* (tumor/normal ratio >2) were observed in 4 of the 18 GCs (22%).

Immunohistochemical Analysis of Connexin 30 in GC

Quantitative RT-PCR revealed obvious *connexin 30* expression in GC, although the levels were not very high. We therefore performed immunohistochemical analysis of connexin 30 in GC (fig. 2a–e). At first, we tested the specificity of the anti-connexin 30 antibody. Immunohistochemical analysis of normal skin tissue was performed, and connexin 30 was detected in the keratinocytes of the upper spinous layers and in those of the stratum granulosum (fig. 2f). This result was consistent with a previous report [49]. Using this antibody, we performed immunostaining of connexin 30 in 169 GCs and the corresponding nonneoplastic gastric mucosa. As a result, connexin 30 expression was detected in 47 of the 169 GCs (28%) and was seen on the cell membrane, especially the apical membrane (fig. 2a, b). However, we sometimes observed its cytoplasmic accumulation (fig. 2c). There was no difference in connexin 30 expression levels between intratumor areas and infiltrative margins.

Connexin 30 was scarcely expressed in any corresponding nonneoplastic gastric mucosa or intestinal metaplasia. Next, we analyzed the relationship between connexin 30 expression and clinicopathologic characteristics. The expression of connexin 30 was observed more frequently in the differentiated type of GC than in the undifferentiated type ($p < 0.0001$) (table 1). Localized distribution of connexin 30-positive GC cells in tumors that had more than 1 histological component were also often observed in differentiated GC components rather than in undifferentiated components.

Furthermore, connexin 30 staining showed a significant inverse correlation with the depth of invasion ($p < 0.0001$), lymph node metastasis ($p = 0.0123$), and TNM stage ($p = 0.0014$). There was no significant association between connexin 30 staining and other parameters (age, gender, or M grade).

Association between Connexin 30 Expression and Gastric/Intestinal Mucin Markers

We next investigated the association between connexin 30 expression and various markers determining the

Table 2. Relationship between connexin 30 expression and gastric/intestinal mucin markers in 169 GC cases

	Connexin 30 expression		p value
	positive (n = 47)	negative (n = 122)	
MUC5AC			
Positive	17 (21)	63	NS
Negative	30 (34)	59	
MUC6			
Positive	13 (39)	20	NS
Negative	34 (25)	102	
MUC2			
Positive	33 (55)	27	<0.0001
Negative	14 (13)	95	
CD10			
Positive	14 (40)	21	NS
Negative	33 (25)	101	

Figures in parentheses are percentages. p values were calculated by Fisher's exact test. NS = Not significant.

gastric/intestinal phenotypes. Out of the 169 cases examined, each molecule was detected in 80 (47%) cases for MUC5AC, 33 (20%) cases for MUC6, 60 (36%) cases for MUC2, and 35 (21%) cases for CD10. The 169 GC cases were classified into 4 phenotypes: 50 (30%) were the gastric phenotype, 41 (24%) were the gastric and intestinal mixed phenotype, 42 (25%) were the intestinal phenotype, and 36 (21%) were the unclassified phenotype. The positive expression of connexin 30 was significantly more frequent in MUC2-positive cases than in MUC2-negative cases ($p < 0.0001$) (table 2). In immunohistochemical staining, the localized distribution of connexin 30 and MUC2 was partly contiguous (fig. 2c, d). Double immunohistochemical staining, however, did not show a coexpression of connexin 30 with MUC2 in any of the tumor cells (fig. 2e). On the other hand, there was no clear relationship between the expression of connexin 30 and other markers (MUC5AC, MUC6, and CD10) (table 2). Connexin 30 expression occurred more frequently in the intestinal phenotype (48%) than in other phenotypes (21%) of GC ($p = 0.0015$) (fig. 2g).

Discussion

Evidence of altered connexin expression in various human malignancies has been accumulating. With regard to the function of connexin in carcinogenesis, there have been several reports of inhibitory effects on the growth of cancer cells [50–53], and transfection and the forced expression of connexin 30 in glioma cell lines has been reported to induce the suppression of tumor growth in vitro [54, 55]. In the present study, we found that approximately 30% of GC cases displayed connexin 30 expression, while nonneoplastic gastric mucosa did not express connexin 30. Furthermore, there was a significant inverse association between connexin 30 expression and tumor progression. Once malignant formation is completed, connexin 30 might inhibit GC cell growth and invasion. In addition, we observed a significant inverse association between connexin 30 expression and the presence of metastasis in the regional lymph nodes. Saunders et al. [56], studying the correlation between the metastatic potential of breast cancer cells and gap junctional communication, showed that the disruption of homospecific or heterospecific GJIC contributes to metastatic potential, but mechanisms by which altered connexin expression and GJIC might contribute to this process are unclear and require future studies. Based on our results, we suggest that the aberrant expression of connexin 30 in GC might not play a role in the metastatic efficiency of malignant cells. The present study showed a higher expression of connexin 30 in the differentiated type of GC compared with the undifferentiated type. This may reflect a loss of the ability to produce this protein along with a decrease in histological differentiation in neoplastic cells. Furthermore, in some cases of GC, we observed a cytoplasmic staining pattern of connexin 30. Previous studies reported that connexin 26 translocated from the cell membrane to the cytoplasm in tumor cells [30, 33]. Furthermore, human connexin 26 and connexin 30 were reported to form functional heteromeric and heterotypic channels [57]. These findings suggest that altered expressions of connexin 30 such as a decrease in functional gap junctions and changed localization of connexin 30 are early events during the development of GC. Although the precise function of cytoplasmic connexin 30 is as yet unclear, one possibility is that the cytoplasmic accumulation of connexin 30 may be a prerequisite for the execution of its role in the cell membrane, contributing to GJIC as needed.

In the present study, the positive expression of connexin 30 showed significant correlation with the positive expression of MUC2. However, there is no previous report showing a direct association between connexin 30 and MUC2. Goblet cells in intestinal metaplasia were positive for MUC2, but scarcely expressed connexin 30. Yamamoto et al. [58] previously reported that connexin

32 might be controlled at the transcriptional level via CDX2. Therefore, connexin 30 might also be regulated by CDX2 and displayed the intestinal phenotype of GC. Further studies should be performed in the near future to elucidate a role for CDX2 in the regulation of connexin 30 in GC.

In summary, we revealed that GC with connexin 30 expression demonstrates an intestinal phenotype that is significantly MUC2-positive in expression. Connexin 30 may be a novel differentiation marker mediating the biological behavior of the intestinal phenotype of GC.

Acknowledgements

We thank Ms. Emiko Hisamoto and Mr. Shinichi Norimura for their excellent technical assistance and advice. This work was carried out with the kind cooperation of the Research Center for Molecular Medicine of the Faculty of Medicine of Hiroshima University. We also thank the Analysis Center of Life Science of Hiroshima University for the use of their facilities. This work was supported in part by grants-in-aid for Cancer Research from the Ministry of Education, Culture, Science, Sports and Technology of Japan and in part by a grant-in-aid for the Third Comprehensive 10-Year Strategy for Cancer Control and for Cancer Research from the Ministry of Health, Labor and Welfare of Japan.

References

1 Ohgaki H, Matsukura N: Stomach cancer; in Stewart BW, Kleihues P (eds): World Cancer Report. Lyon, IARC Press, 2003, p 197.
2 Yasui W, Yokozaki H, Fujimoto J, Naka K, Kuniyasu H, Tahara E: Genetic and epigenetic alterations in multistep carcinogenesis of the stomach. J Gastroenterol 2000;35:111–115.
3 Ushijima T, Sasako M: Focus on gastric cancer. Cancer Cell 2004;5:121–125.
4 Yasui W, Oue N, Ito R, Kuraoka K, Nakayama H: Search for new biomarkers of gastric cancer through serial analysis of gene expression and its clinical implications. Cancer Sci 2004;95:385–392.
5 Lockhart DJ, Dong H, Byrne MC, et al: Expression monitoring by hybridization to high-density oligonucleotide arrays. Nat Biotechnol 1996;14:1675–1680.
6 Velculescu VE, Zhang L, Vogelstein B, Kinzler KW: Serial analysis of gene expression. Science 1995;270:484–487.
7 Lauren P: The two histological main types of gastric carcinoma: diffuse and so-called intestinal-type carcinoma. An attempt at a histo-clinical classification. Acta Pathol Microbiol Scand 1965;64:31–49.
8 Nakamura K, Sugano H, Takagi K: Carcinoma of the stomach in incipient phase: its histogenesis and histological appearances. Gann 1968;59:251–258.
9 Saito K, Shimoda T: The histogenesis and early invasion of gastric cancer. Acta Pathol Jpn 1986;36:1307–1318.
10 Tahara E: Genetic alterations in human gastrointestinal cancers: the application to molecular diagnosis. Cancer 1995;75:1410–1417.
11 Tatematsu M, Ichinose M, Miki K, Hasegawa R, Kato T, Ito N: Gastric and intestinal phenotypic expression of human stomach cancers as revealed by pepsinogen immunohistochemistry and mucin histochemistry. Acta Pathol Jpn 1990;40:494–504.
12 Yoshikawa A, Inada Ki K, Yamachika T, Shimizu N, Kaminishi M, Tatematsu M: Phenotypic shift in human differentiated gastric cancers from gastric to intestinal epithelial cell type during disease progression. Gastric Cancer 1998;1:134–141.
13 Tajima Y, Yamazaki K, Nishino N, et al: Gastric and intestinal phenotypic marker expression in gastric carcinomas and recurrence pattern after surgery – immunohistochemical analysis of 213 lesions. Br J Cancer 2004;91:1342–1348.
14 Saito A, Shimoda T, Nakanishi Y, Ochiai A, Toda G: Histologic heterogeneity and mucin phenotypic expression in early gastric cancer. Pathol Int 2001;51:165–171.
15 Kabashima A, Yao T, Sugimachi K, Tsuneyoshi M: Relationship between biologic behavior and phenotypic expression in intramucosal gastric carcinomas. Hum Pathol 2002;33:80–86.
16 Shibata N, Watari J, Fujiya M, Tanno S, Saitoh Y, Kohgo Y: Cell kinetics and genetic instabilities in differentiated type early gastric cancers with different mucin phenotype. Hum Pathol 2003;34:32–40.
17 Tsukashita S, Kushima R, Bamba M, Sugihara H, Hattori T: MUC gene expression and histogenesis of adenocarcinoma of the stomach. Int J Cancer 2001;94:166–170.
18 Wakatsuki K, Yamada Y, Narikiyo M, et al: Clinicopathological and prognostic significance of mucin phenotype in gastric cancer. J Surg Oncol 2008;98:124–129.
19 Yuasa Y: Control of gut differentiation and intestinal-type gastric carcinogenesis. Nat Rev Cancer 2003;3:592–600.
20 Mizoshita T, Tsukamoto T, Nakanishi H, et al: Expression of Cdx2 and the phenotype of advanced gastric cancers: relationship with prognosis. J Cancer Res Clin Oncol 2003;129:727–734.
21 Tsukamoto T, Inada K, Tanaka H, et al: Down-regulation of a gastric transcription factor, Sox2, and ectopic expression of intestinal homeobox genes, Cdx1 and Cdx2: inverse correlation during progression from gastric/intestinal-mixed to complete intestinal metaplasia. J Cancer Res Clin Oncol 2004;130:135–145.
22 Evans WH, Martin PE: Gap junctions: structure and function (Review). Mol Membr Biol 2002;19:121–136.
23 Kumar NM, Gilula NB: The gap junction communication channel. Cell 1996;84:381–388.
24 Goodenough DA, Goliger JA, Paul DL: Connexins, connexons, and intercellular communication. Annu Rev Biochem 1996;65:475–502.
25 Janssen-Timmen U, Traub O, Dermietzel R, Rabes HM, Willecke K: Reduced number of gap junctions in rat hepatocarcinomas detected by monoclonal antibody. Carcinogenesis 1986;7:1475–1482.
26 Mesnil M: Connexins and cancer. Biol Cell 2002;94:493–500.
27 Muramatsu A, Iwai M, Morikawa T, et al: Influence of transfection with connexin 26 gene on malignant potential of human hepatoma cells. Carcinogenesis 2002;23:351–358.
28 Tanaka M, Grossman HB: Connexin 26 gene therapy of human bladder cancer: induction of growth suppression, apoptosis, and synergy with Cisplatin. Hum Gene Ther 2001;12:2225–2236.
29 Villaret DB, Wang T, Dillon D, et al: Identification of genes overexpressed in head and neck squamous cell carcinoma using a combination of complementary DNA subtraction and microarray analysis. Laryngoscope 2000;110:374–381.
30 Kanczuga-Koda L, Sulkowski S, Koda M, Sulkowska M: Alterations in connexin26 expression during colorectal carcinogenesis. Oncology 2005;68:217–222.

31 Tate AW, Lung T, Radhakrishnan A, Lim SD, Lin X, Edlund M: Changes in gap junctional connexin isoforms during prostate cancer progression. Prostate 2006;66:19–31.
32 Kyo N, Yamamoto H, Takeda Y, et al: Overexpression of connexin 26 in carcinoma of the pancreas. Oncol Rep 2008;19:627–631.
33 Jamieson S, Going JJ, D'Arcy R, George WD: Expression of gap junction proteins connexin 26 and connexin 43 in normal human breast and in breast tumours. J Pathol 1998; 184:37–43.
34 Kanczuga-Koda L, Sulkowski S, Lenczewski A, et al: Increased expression of connexins 26 and 43 in lymph node metastases of breast cancer. J Clin Pathol 2006;59:429–433.
35 Dahl E, Manthey D, Chen Y, et al: Molecular cloning and functional expression of mouse connexin-30, a gap junction gene highly expressed in adult brain and skin. J Biol Chem 1996;271:17903–17910.
36 Lautermann J, Frank HG, Jahnke K, Traub O, Winterhager E: Developmental expression patterns of connexin26 and -30 in the rat cochlea. Dev Genet 1999;25:306–311.
37 Nagy JI, Patel D, Ochalski PA, Stelmack GL: Connexin30 in rodent, cat and human brain: selective expression in gray matter astrocytes, co-localization with connexin43 at gap junctions and late developmental appearance. Neuroscience 1999;88:447–468.
38 Grifa A, Wagner CA, D'Ambrosio L, et al: Mutations in GJB6 cause nonsyndromic autosomal dominant deafness at DFNA3 locus. Nat Genet 1999;23:16–18.
39 del Castillo I, Villamar M, Moreno-Pelayo MA, et al: A deletion involving the connexin 30 gene in nonsyndromic hearing impairment. N Engl J Med 2002;346:243–249.
40 Smith FJ, Morley SM, McLean WH: A novel connexin 30 mutation in Clouston syndrome. J Invest Dermatol 2002;118:530–532.
41 Ozawa H, Matsunaga T, Kamiya K, et al: Decreased expression of connexin-30 and aberrant expression of connexin-26 in human head and neck cancer. Anticancer Res 2007; 27:2189–2195.
42 Aasen T, Graham SV, Edward M, Hodgins MB: Reduced expression of multiple gap junction proteins is a feature of cervical dysplasia. Mol Cancer 2005;4:31.
43 Haass NK, Wladykowski E, Kief S, Moll I, Brandner JM: Differential induction of connexins 26 and 30 in skin tumors and their adjacent epidermis. J Histochem Cytochem 2006;54:171–182.
44 Japanese Gastric Cancer Association: Japanese Classification of Gastric Carcinoma, ed 13. Tokyo, Kanehara, 1995.
45 Sobin LH, Wittekind CH (eds): TNM Classification of Malignant Tumors, ed 6. New York, Wiley, 2002, pp 65–68.
46 Gibson UE, Heid CA, Williams PM: A novel method for real time quantitative RT-PCR. Genome Res 1996;6:995–1001.
47 Kondo T, Oue N, Yoshida K, et al: Expression of POT1 is associated with tumor stage and telomere length in gastric carcinoma. Cancer Res 2004;64:523–529.
48 Oue N, Mitani Y, Aung PP, et al: Expression and localization of Reg IV in human neoplastic and non-neoplastic tissues: Reg IV expression is associated with intestinal and neuroendocrine differentiation in gastric adenocarcinoma. J Pathol 2005;207:185–198.
49 Essenfelder GM, Bruzzone R, Lamartine J, et al: Connexin30 mutations responsible for hidrotic ectodermal dysplasia cause abnormal hemichannel activity. Hum Mol Genet 2004; 13:1703–1714.
50 Zhu D, Kidder GM, Caveney S, Naus CC: Growth retardation in glioma cells cocultured with cells overexpressing a gap junction protein. Proc Natl Acad Sci USA 1992; 89:10218–10221.
51 Goldberg GS, Bechberger JF, Tajima Y, et al: Connexin43 suppresses MFG-E8 while inducing contact growth inhibition of glioma cells. Cancer Res 2000;60:6018–6026.
52 Seul KH, Kang KY, Lee KS, Kim SH, Beyer EC: Adenoviral delivery of human connexin37 induces endothelial cell death through apoptosis. Biochem Biophys Res Commun 2004;319:1144–1151.
53 Moorby C, Patel M: Dual functions for connexins: Cx43 regulates growth independently of gap junction formation. Exp Cell Res 2001;271:238–248.
54 Princen F, Robe P, Gros D, et al: Rat gap junction connexin-30 inhibits proliferation of glioma cell lines. Carcinogenesis 2001;22: 507–513.
55 Mennecier G, Derangeon M, Coronas V, Herve JC, Mesnil M: Aberrant expression and localization of connexin43 and connexin30 in a rat glioma cell line. Mol Carcinog 2008;47:391–401.
56 Saunders MM, Seraj MJ, Li Z, et al: Breast cancer metastatic potential correlates with a breakdown in homospecific and heterospecific gap junctional intercellular communication. Cancer Res 2001;61:1765–1767.
57 Yum SW, Zhang J, Valiunas V, et al: Human connexin26 and connexin30 form functional heteromeric and heterotypic channels. Am J Physiol Cell Physiol 2007;293:1032–1048.
58 Yamamoto T, Kojima T, Murata M, et al: IL-1beta regulates expression of Cx32, occludin, and claudin-2 of rat hepatocytes via distinct signal transduction pathways. Exp Cell Res 2004;299:427–441.

Pathology International 2010; **60**: 673–680 doi:10.1111/j.1440-1827.2010.02587.x

Original Article

Immunohistochemical analysis of colorectal cancer with gastric phenotype: Claudin-18 is associated with poor prognosis

Miho Matsuda,[1] Kazuhiro Sentani,[1] Tsuyoshi Noguchi,[2] Takao Hinoi,[3] Masazumi Okajima,[3] Keisuke Matsusaki,[4] Naoya Sakamoto,[1] Katsuhiro Anami,[1] Yutaka Naito,[1] Naohide Oue[1] and Wataru Yasui[1]

[1]Department of Molecular Pathology, [3]Department of Endoscopic Surgery and Surgical Science, Hiroshima University Graduate School of Biomedical Sciences, Hiroshima, [2]Department of Gastrointestinal Surgery, Oita University Faculty of Medicine, Oita and [4]Department of Surgery, Hofu Institute of Gastroenterology, Hofu, Japan

Claudin-18 plays a key role in constructing tight junctions, and altered claudin-18 expression has been documented in various human malignancies; however, little is known about the biological significance of claudin-18 in colorectal cancer (CRC). The aim of this study is to investigate the significance of claudin-18 expression in CRC and its association with clinicopathological factors. We performed clinicopathological analysis of claudin-18 expression in a total of 569 CRCs by immunohistochemistry. Moreover, we investigated the association between claudin-18 and various markers including gastric/intestinal phenotype (MUC5AC, MUC6, MUC2 and CD10), CDX2, claudin-3, claudin-4, p53 and Ki-67.

Claudin-18 expression was detected in 21 of the 569 CRCs (4%) and was seen exclusively on the cell membrane. Positive expression of claudin-18 showed a significant correlation with positive expression of MUC5AC ($P < 0.0001$) and negative expression of CDX2 ($P = 0.0013$). The prognosis of patients with positive claudin-18 expression was significantly poorer than in negative cases ($P = 0.0106$). Multivariate analysis revealed that T grade, M grade and claudin-18 expression were independent predictors of survival in patients with CRC. We revealed that claudin-18 expression correlates with poor survival in patients with CRC and is associated with the gastric phenotype.

Key words: claudin-18, colorectal cancer, gastric phenotype, MUC5AC, prognosis

Correspondence: Wataru Yasui, MD, PhD, Department of Molecular Pathology, Hiroshima University Graduate School of Biomedical Sciences, 1-2-3 Kasumi, Minami-ku, Hiroshima 734-8551, Japan. Email: wyasui@hiroshima-u.ac.jp

Received 28 February 2010. Accepted for publication 20 June 2010.

Colorectal cancer (CRC) is one of the most common malignancies worldwide, and its incidence has increased in recent years.[1] Several molecules associated with carcinogenesis and tumor progression have been identified;[2–4] however, these mechanisms remain unclear.

Claudin proteins, a family of proteins comprising at least 24 members, are components of tight junction strands that regulate paracellular transport and lateral diffusion of membrane lipids and proteins.[5] Claudins are expressed in an organ-specific manner. Claudin-18 has two alternatively spliced variants in mice: variant 1 (claudin-18a1) is expressed in the lung, whereas variant 2 (claudin-18a2) is expressed in the stomach.[6] In normal human tissues, expression of claudin-18a2 is confined to gastric epithelial cells (foveolar, endocrine, parietal, and chief cells) and duodenal Paneth cells,[7] and not in other organs including esophagus, colon, pancreas, lung, and so on.[8] However, altered claudin-18 expression has been documented in various diseases. Expression of claudin-18 is increased in both experimental colitis and human inflammatory bowel disease.[9] Frequent ectopic activation of claudin-18 was reported in pancreatic, esophageal, ovarian, and lung tumors, using quantitative reverse transcription-PCR.[8] We previously reported that expression of claudin-18 is retained in about half of gastric cancers, which correlated with a survival benefit.[7] In addition, we showed ectopic expression of claudin-18 in signet ring cell carcinoma of CRC.[10] However, little is known about the clinicopathological significance of claudin-18 in CRC. Moreover, claudin-3 and claudin-4 were reported to express in normal colon mucosa and CRC.[11,12] Claudin-18 has been defined as gastric claudin, and claudin-3 and claudin-4 as intestinal claudin in gastric cancer, and it has been reported that classification of gastric cancers using gastric and intestinal claudins is a good biomarker for assessing the risk of poor prognosis.[13]

Mucin genes have been shown to be altered in various epithelial cancers,[14] and gastric cancers are classified as having a gastric, gastric and intestinal mixed, or intestinal phenotype depending on the expression of mucin phenotypic markers.[15–17] Aberrant expression of mucin genes has also been observed in CRC.[14,18,19] Patients with long-standing ulcerative colitis (UC) are at a high risk of development of CRC,[20] and MUC5AC and MUC6 are expressed in UC-associated CRC.[21] It has also been reported that MUC5AC expression was observed during colon carcinogenesis in rats.[22] Furthermore, MUC5AC expression has been reported to be associated with poor prognosis.[23]

The caudal homeobox 2 gene (CDX2) is a homeobox transcription factor that plays a master role in intestinal differentiation and homeostasis in the colon.[24] About 85% of CRCs express CDX2 immunohistochemically, and this is inversely associated with tumor stage.[25]

The present study represents the first detailed analysis of claudin-18 expression in CRC. To clarify the pattern of expression and localization of claudin-18 in CRC, we performed immunohistochemical analysis of surgically resected CRC samples. In addition, we investigated the association between claudin-18 and various markers including gastric/intestinal phenotype (MUC5AC, MUC6, MUC2, CD10), CDX2, other claudins (claudin-3 and claudin-4), p53 and Ki-67. Furthermore, we also evaluated the relationship between claudin-18 expression and patients' prognosis.

MATERIALS AND METHODS

Tissue samples

Primary tumor samples were collected from 569 patients with CRC (305 men and 264 women; age range, 46–93 years; mean, 68 years). Patients were treated at the Hiroshima University Hospital, Hiroshima, Japan, or affiliated hospitals. For immunohistochemical analysis, we used archival formalin-fixed, paraffin-embedded tissues from 569 patients who had undergone surgical excision for CRC. The 569 CRC cases included 395 samples on a tissue microarray (TMA) using a Tissue Microarrayer (AZUMAYA KIN-1, Tokyo, Japan). The two most representative tumor areas to be sampled for the TMAs were carefully selected in each case. The 569 CRC cases were histologically classified as 308 well differentiated, 246 moderately differentiated, 11 poorly differentiated, and 4 mucinous adenocarcinomas, according to the World Health Organization (WHO) classification.[26] Tumor staging was carried out according to the TNM classification[27] and Dukes' classification. Information on patient survival was available for 97 patients with advanced CRC (Dukes' stage B to C). Because written informed consent was not obtained, identifying information for all samples was removed before analysis for strict privacy protection. This procedure was in accordance with the Ethical Guidelines for Human Genome/Gene Research enacted by the Japanese Government.

Antibodies

Anti-claudin-18 antibody (C-term) was purchased from Invitrogen/Zymed Laboratories Inc. (San Francisco, CA, USA). This antibody was the same as that used in our previous study,[7] and recognizes only claudin-18a2. We used four antibodies for analysis of the CRC phenotypes: anti-MUC5AC (Novocastra, Newcastle, UK) as a marker of gastric foveolar epithelial cells, anti-MUC6 (Novocastra) as a marker of pyloric gland cells, anti-MUC2 (Novocastra) as a marker of goblet cells in the small intestine and colorectum, anti-CD10 (Novocastra) as a marker of microvilli of absorptive cells in the small intestine and colorectum. We used anti-CDX2 (BioGenex, San Ramon, CA, USA) as a marker of differentiation of intestinal epithelial cells, anti-Ki-67 (Dako, Carpinteria, CA, USA), and anti-p53 (Novocastra). Furthermore, anti-claudin-3 and anti-claudin-4 antibodies were purchased from Invitrogen/Zymed Laboratories Inc.

Immunohistochemistry

A Dako LSAB Kit (Dako) was used for immunohistochemical analysis. In brief, sections were pretreated by microwave treatment in citrate buffer for 15 min to retrieve antigenicity. After peroxidase activity was blocked with 3% H_2O_2-methanol for 10 min, sections were incubated with normal goat serum (Dako) for 20 min to block non-specific antibody binding sites. Sections were incubated with the following primary antibodies: anti-claudin-18 (diluted 1:50), anti-MUC5AC (1:50), anti-MUC6 (1:50), anti-MUC2 (1:50), anti-CD10 (1:50), anti-CDX2 (1:20), anti-claudin-3 (1:50), anti-claudin-4 (1:50), anti-Ki-67 (1:50) and anti-p53 (1:50). Sections were incubated with primary antibody for 1 h at 25°C, followed by incubations with biotinylated anti-rabbit/mouse IgG and peroxidase labelled streptavidin for 10 min each. Staining was completed with a 10-min incubation with the substrate-chromogen solution. The sections were counterstained with 0.1% haematoxylin.

Claudin-18, CDX2 and p53 staining was classified according to the percentage of stained cancer cells. Expression was considered to be 'negative' if <10% of cancer cells were stained. When at least 10% of cancer cells were stained, the result of immunostaining was considered 'positive.' Expression of claudin-3 and claudin-4 was considered to be 'reduced' if less than 50% of cancer cells were stained. When at least 50% of cancer cells were stained, the immunostain-

ing was considered 'preserved'. Ki-67 expression was classified into two groups according to the percentage of stained cancer cells.

The CRC cases were classified into four phenotypes: gastric phenotype, intestinal phenotype, gastric and intestinal mixed phenotype, and unclassified phenotype. The criteria[28] for classification of gastric phenotype and intestinal phenotype were as follows. The CRCs in which more than 10% of the cells displayed the gastric or intestinal epithelial cell phenotype were gastric phenotype or intestinal phenotype cancers, respectively. Those sections that showed both gastric and intestinal phenotypes were classified as gastric and intestinal mixed phenotype, and those that lacked both the gastric and the intestinal phenotypes were classified as unclassified phenotype.

For the TMAs, staining was also considered positive on the same basis as described above.

Double immunofluorescence staining

Double-immunofluorescence staining was performed as described previously.[29] Alexa Fluor 488-conjugated chicken anti-rabbit IgG and Alexa Fluor 546-conjugated goat anti-mouse IgG were used as secondary antibodies (Molecular Probes, Eugene, OR, USA).

Statistical methods

Correlations between clinicopathologic parameters and claudin-18 staining were analyzed by Fisher's exact test. Kaplan-Meier survival curves were constructed for claudin-18, MUC5AC, MUC6, MUC2, CD10 or CDX2-positive and -negative patients to compare survival between both groups. The differences in survival curves between groups were tested for statistical significance by the log-rank test.[30] Cox proportional hazards multivariate model was used to examine the association of clinicopathologic factors and the expression of claudin-18 with survival. A *P*-value of less than 0.05 was considered statistically significant.

RESULTS

Immunohistochemical analysis of claudin-18 in CRC

We performed immunostaining of claudin-18 in CRC. Claudin-18 expression was detected in 21 of the 569 CRCs (4%) and was seen exclusively on the cell membrane (Fig. 1a). There was no difference in claudin-18 expression levels between intratumor areas and infiltrative margins, and in the presence or absence of vessel infiltration. Corresponding non-neoplastic colorectal mucosa and adenomas of the colon did not express claudin-18. Next, we analyzed the relationship between claudin-18 expression and clinicopathologic characteristics. Expression of claudin-18 was not correlated with T grade, N grade, tumor staging, or histological type (Table 1).

Association of expression between claudin-18 and various molecules including mucins, CDX2, other claudins, p53 and Ki-67

We next investigated the association between claudin-18 expression and various markers determining gastric/intestinal phenotype. Out of the 569 cases examined, each molecule was detected in 86 (15%) cases for MUC5AC, 11 (2%) cases for MUC6, 370 (65%) cases for MUC2, 200 (35%) cases for CD10. 569 CRC cases were classified into four phenotypes: 14 (2%) gastric phenotype, 76 (13%) gastric and intestinal mixed phenotype, 389 (68%) intestinal phenotype, and 90 (16%) unclassified phenotype. Positive expression of claudin-18 was significantly more frequent in MUC5AC-positive cases than MUC5AC-negative cases ($P < 0.0001$) (Table 2). In immunohistochemical staining, coexpression of claudin-18 and MUC5AC was often detected (Fig. 1a,b). Double-immunohistochemical staining also showed coexpression of claudin-18 with MUC5AC in many tumor cells (Fig. 1c). On the other hand, CDX2 was detected in 448 of the 569 (79%) cases, and positive expression of claudin-18 was significantly more frequent in CDX2-negative cases than CDX2-positive cases ($P = 0.0013$) (Table 2). There was no clear relationship between expression of claudin-18 and other markers (MUC6, MUC2, CD10, Ki-67 and p53) (Table 2). Moreover, positive expression of claudin-18 (gastric claudin) also showed no significant correlation with reduced expression of claudin-3 and claudin-4 (intestinal claudin).

Morphological characteristics of claudin-18-positive-MUC5AC-positive CRC in comparison with claudin-18-negative-MUC5AC-positive CRC

Furthermore, we analyzed morphological differences between 13 claudin and 18-positive-MUC5AC-positive CRC cases and 73 claudin-18-negative-MUC5AC-positive CRC cases. In the former, 6 of the 13 (46%) cases showed cohesive and microglandular structures with scant cytoplasm and nuclear atypia (Fig. 1d,e). They resembled gastric tubular adenocarcinoma in appearance, the components of which also showed gastric phenotype immunohistochemically. In the latter, only 5 of the 73 (7%) cases showed such struc-

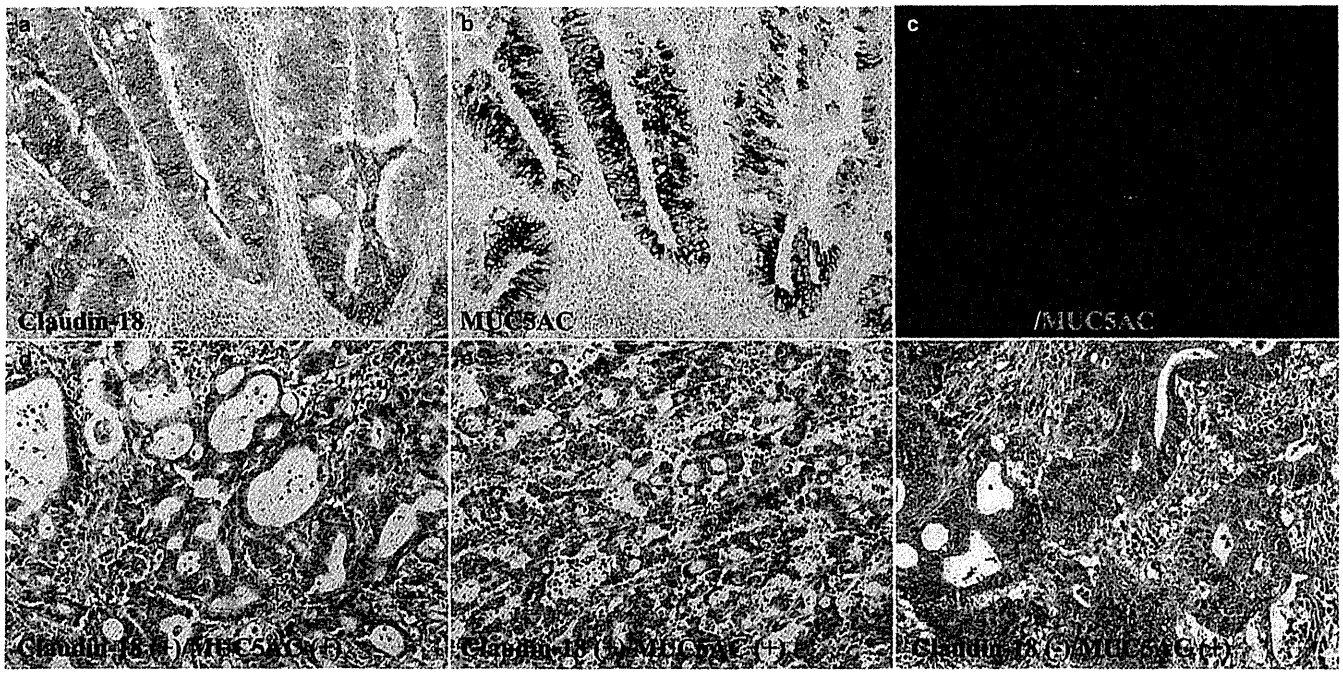

Figure 1 Immunohistochemical staining of claudin-18 and MUC5AC in colorectal cancer (CRC) tissues. (**a**) Immunohistochemistry of claudin-18. Claudin-18 was detected in cell membranes. (**b**) Immunohistochemistry of MUC5AC. MUC5AC was detected in the cytoplasm. (**c**) Double-immunostaining of claudin-18 (red) and MUC5AC (green). Nuclei are stained with 4; 6-diamidino-2-phenylindole (DAPI; blue). (**d,e**) Some of claudin-18-positive-MUC5AC-positive CRC showed cohesive and microglandular structures with scant cytoplasm and nuclear atypia. The resemblance to gastric tubular adenocarcinoma is remarkable. (**f**) Most of claudin-18-negative-MUC5AC-positive CRC revealed irregular formation of glands with relatively abundant and eosinophilic cytoplasm, prominent nuclei and loss of polarity. Original magnification: (**a,b,d–f**) × 200; (**c**) × 800.

tures, and remaining cases revealed common form of conventional CRC which have irregular formation of glands with relatively abundant and eosinophilic cytoplasm, prominent nuclei and loss of polarity (Fig. 1f).

Relationship between expression of claudin-18, mucins and CDX2 in CRC and patients' prognosis

We also examined the relationship between survival and expression of claudin-18, mucins and CDX2 in advanced CRC (Dukes' stage B to C, $n = 97$). The prognosis of patients with positive claudin-18 or MUC5AC expression was significantly poorer than in the negative cases ($P = 0.0106$ or $P = 0.0462$, respectively, log-rank test) (Fig. 2a,b). In contrast, the prognosis of patients with negative CDX2 expression was significantly poorer than in the positive cases ($P = 0.0044$, log-rank test) (Fig. 2c). The percentage of claudin-18 positive area within CRC between >50% and 10–50% showed no significant difference in prognosis. In the meantime, the prognosis of patients with positive MUC2 or CD10 expression was not significantly poorer than in the negative cases. Next, the Cox proportional hazards multivariate model was used to examine the association of clinicopathologic factors and the expression of claudin-18 with survival. Multivariate analysis revealed that T grade, M grade and claudin-18 expression were independent predictors of survival in patients with CRC (Table 3).

DISCUSSION

Evidence of altered claudin expression in various human malignancies has been accumulating. In ovarian cancer, claudin-3 and claudin-4 proteins are highly overexpressed[31] and overexpression of these claudins increases cell invasion and motality,[32] whereas reduced or loss of expression of claudin family members has been found to promote cell invasion and metastasis in malignant tumors, including those of the breast,[33] pancreas[34] and gastrointestinal tract.[12] Ectopic expression of claudin-18 in CRC has also been reported recently.[8,10] However, little is known about the biological significance of claudin-18 in CRC. We previously reported that retained claudin-18 was correlated with a survival benefit in gastric cancer.[7] In the present study, however, ectopic expression of claudin-18 in CRC was correlated with poor survival. Seemingly, this result contradicts the previous analysis in gastric cancer. Claudin family members are crucial components of tight junction, and exhibit highly tissue specific patterns.[35] In gastric cancer, down-regulation of

Table 1 Relationship between claudin-18 expression and clinicopathologic parameters in 569 CRC cases

	Claudin-18 expression		
	Positive	Negative	*P* value*
Age			
≤65 years	9 (3%)	263	NS
>65 years	12 (4%)	285	
Sex			
Male	10 (3%)	295	NS
Female	11 (4%)	253	
Tumor location			
Right/transverse	8 (4%)	190	NS
Left/sigmoid/rectum	13 (4%)	358	
T grade†			
Tis/T1/T2	7 (5%)	135	NS
T3/T4	14 (3%)	413	
N grade†			
N0	14 (4%)	344	NS
N1/2	7 (3%)	204	
M grade†			
M0	20 (4%)	518	NS
M1	1 (3%)	30	
Stage†			
0/I/II	14 (4%)	335	NS
III/IV	7 (3%)	213	
Histologic type‡			
Well/moderately	19 (3%)	535	NS
Poorly/mucinous	2 (13%)	13	

*Fisher's exact test.

†Tumor stage was classified according to the criteria of the International Union Against Cancer TNM classification of malignant tumors.

‡Histology was according to the World Health Organization (WHO) classification.

CRC, colorectal cancer; NS, not significant.

Table 2 Relationship between claudin-18 expression and various markers in CRC cases

	Claudin-18 expression		
	Positive	Negative	*P* value*
MUC5AC (569)			
Positive	13 (15%)	73	<0.0001
Negative	8 (2%)	475	
MUC6 (569)			
Positive	2 (18%)	9	NS
Negative	19 (3%)	539	
MUC2 (569)			
Positive	18 (5%)	352	NS
Negative	3 (2%)	196	
CD10 (569)			
Positive	4 (2%)	196	NS
Negative	17 (5%)	352	
CDX2 (569)			
Positive	10 (2%)	438	0.0013
Negative	11 (9%)	110	
Claudin-3 (569)			
Reduced	7 (3%)	213	NS
Preserved	14 (4%)	335	
Claudin-4 (569)			
Reduced	10 (3%)	283	NS
Preserved	11 (4%)	265	
Ki-67 (63)			
>50%	7 (37%)	12	NS
0–50%	14 (32%)	30	
p53 (63)			
Positive	12 (32%)	25	NS
Negative	9 (35%)	17	

*Fisher's exact test.

CDX2, caudal-related homeobox gene 2; CRC, colorectal cancer; NS, not significant.

claudin-18, which shows orthotopic expression in normal stomach, might lead to poor survival. In the meantime, ectopic expression of claudin-18 in CRC may affect permeability at tight junctions, possibly increasing the diffusion of nutrients and other extracellular growth factors to promote cancer cell growth, survival and motility. There was no significant correlation between frequency of claudin-18 expression and histological type, but poorly differentiated adenocarcinomas also expressed claudin-18. These results indicated that claudin-18 in CRC contributed to tumor promotion rather than simply worked as cell adhesion. It was recently reported that expression of claudin-18 in patients with UC was significantly upregulated as compared to healthy individuals.[9] Ulcerative colitis is associated with an increased risk of developing CRC.[36] In the present study, non-neoplastic colorectal mucosa and adenoma of the colon did not express claudin-18. There was no clear relationship between expression of claudin-18, Ki-67 and p53. Therefore, we speculated that ectopic expression of claudin-18 in the colon might be associated with invasion in tumor progression, but further analyses are required.

We previously revealed that down-regulation of claudin-18 was preferentially observed in gastric cancer with intestinal phenotype.[7] Recently, Yano *et al.* reported that transcriptional activation of the human claudin-18 gene promoter was regulated through activator protein-1 in phorbol 12-myristate 13-acetate treatment of MKN45 gastric cancer cells,[37] which have gastric phenotype.[38] To date, CRC with gastric phenotype has been reported to frequently exhibit lymphatic permeation and lymph node metastasis.[39] Furthermore, MUC5AC expression was reported to be associated with poor prognosis.[23] These are concordant with the present result. However, the biological interaction between claudin-18 and MUC5AC is poorly understood. In addition, it remains unknown why CRC with expression of MUC5AC has poor prognosis. The previous study has shown very low levels of MUC5AC in normal colon,[40] but abnormal expression of MUC5AC during the early stages of colorectal carcinogenesis has been confirmed by several groups using biochemical, immunohistochemical and molecular biology techniques.[40–43]

CDX2 is reported to be involved in colorectal carcinogenesis[44] as well as the status of its differentiation,[45] and is

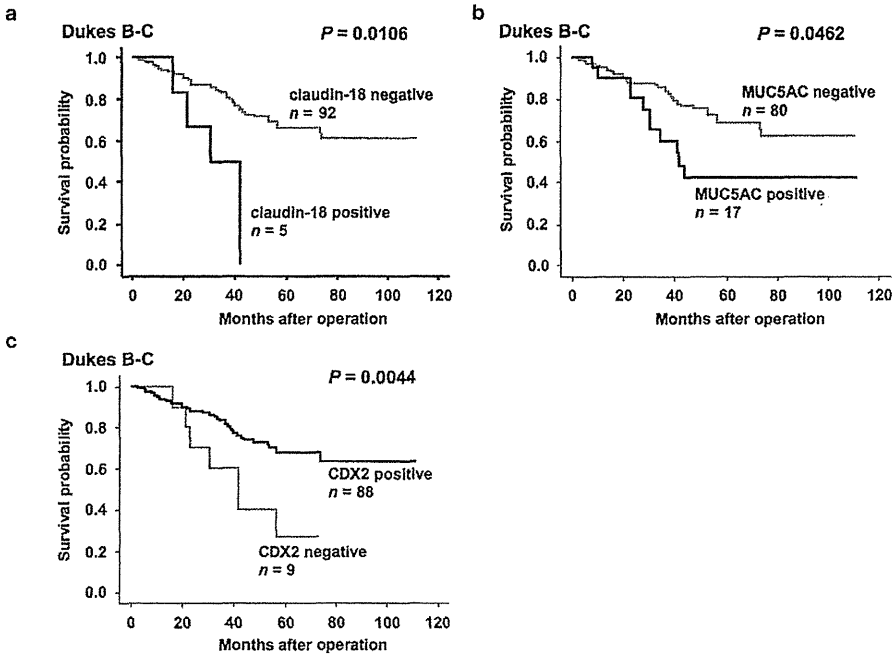

Figure 2 Prognostic value of claudin-18, MUC5AC and CDX2 staining in 97 patients with advanced colorectal cancer (CRC) (Dukes B-C). (**a**) Kaplan–Meier curves of patients with claudin-18-negative or claudin-18-positive CRC. The survival of patients with claudin-18-positive CRC was significantly worse ($P = 0.0106$, log-rank test). (**b**) MUC5AC-negative or MUC5AC-positive CRC. The survival of patients with MUC5AC-positive CRC was significantly worse ($P = 0.0462$, log-rank test). (**c**) CDX2-negative or CDX2-positive CRC. The survival of patients with CDX2-negative CRC was significantly worse ($P = 0.0044$, log-rank test).

Table 3 Multivariate analysis of factors influencing survival in 117 CRC cases

Factor	Hazard ratio	95% CI	χ^2	*P* value
Age				
≤65 years	1	Reference	1.356	NS
>65 years	1.46	0.772–2.761		
Sex				
Female	1	Reference	0.307	NS
Male	1.204	0.625–2.321		
Tumor location				
Right/transverse	1	Reference	0.694	NS
Left/sigmoid/rectum	1.476	0.591–3.689		
T grade†				
Tis/T1/T2	1	Reference	6.565	0.0104
T3/T4	4.999	1.459–17.122		
N grade†				
N0	1	Reference	2.661	NS
N1/2	5.5	0.709–42.625		
M grade†				
M0	1	Reference	4.97	0.0258
M1	2.311	1.106–4.282		
Stage†				
0/I/II	1	Reference	0.062	NS
III/IV	1.326	0.145–12.16		
Histologic type‡				
Well/moderately	1	Reference	1.73	NS
Poorly/mucinous	4.157	0.497–34.738		
Claudin-18				
Negative	1	Reference	5.331	0.0209
Positive	3.603	1.214–10.695		

†Tumor stage was classified according to the criteria of the International Union against Cancer TNM classification of malignant tumors.

‡Histology was according to the World Health Organization (WHO) classification.

NS, not significant.

known to be a tumor suppressor.[46] Down-regulation of CDX2 in CRC was reported to increase throughout tumor progression,[25,46] and expression of CDX2 was reported to reduce the tumorigenesis in CRC cell lines.[47] In the present study, the prognosis of patients with negative CDX2 expression was significantly poorer than patients with positive expression. To date, little is known about the relationship between claudin-18 and CDX2 expression, but Satake *et al.* reported that expression of claudin-18 was not altered by ectopic CDX2 in gastric cancer cell lines.[48] In the present study, positive expression of claudin-18 showed significant correlation with positive expression of MUC5AC and negative expression of CDX2. There might be no direct association between claudin-18, MUC5AC and CDX2. Double-immunohistochemical staining, however, showed coexpression of claudin-18 with MUC5AC in many tumor cells, and these molecules might be controlled by common transcription factors. SOX2 is an HMG-box transcription factor expressed in gastric mucosa but not in intestine. Park *et al.* reported that aberrant expression of SOX2 up-regulated MUC5AC in CRC.[49] In addition, Tsukamoto *et al.* reported that the immunohistochemical expression patterns of SOX2 and CDX2 were inversely related in the human stomach.[50] Further studies should be performed in the near future to elucidate a role for SOX2 in regulation of claudin-18 in CRC.

Morphological analysis revealed that CRC with both claudin-18 and MUC5AC expression are more likely to resemble gastric tubular adenocarcinoma in appearance than CRC with MUC5AC expression alone. Both claudin-18 and MUC5AC show orthotopic expression in normal stomach, and their ectopic expression in CRC may lead to

morphological resemblance to gastric cancer. Colorectal cancer with gastric phenotype is closely associated with specific genetic subtypes, such as microsatellite instability (MSI). CDX2 was also reported to be mutated in CRC with microsatellite instability-high (MSI-H).[51] Colorectal cancer with both claudin-18 and MUC5AC expression in the present study had few typical clinicopathological features of CRC with MSI-H (poorly differentiated or mucinous appearance, often with prominent tumor-infiltrating lymphocytes, and tendency for right side), but further examinations are required.

Indeed TMAs cannot be used to evaluate the heterogeneous expression patterns of various cancer-related molecules, but we examined 569 CRC cases that included 174 samples from surgically resected specimens. Furthermore, use of TMAs to immunophenotype malignant tumors was previously validated by Hoos *et al.* [52] and their data showed an excellent concordance between the results obtained when TMAs were used with triplicate cores per tumor and with full sections. In summary, we revealed that CRC with claudin-18 expression has a poor prognosis and demonstrates a gastric phenotype that is significantly MUC5AC-positive or CDX2-negative in expression. Claudin-18 may be a useful marker to predict CRC with poor prognosis.

ACKNOWLEDGMENTS

We thank Ms. Emiko Hisamoto and Mr Shinichi Norimura for excellent technical assistance and advice. This work was carried out with the kind cooperation of the Research Center for Molecular Medicine, Faculty of Medicine, Hiroshima University. We thank the Analysis Center of Life Science, Hiroshima University, for the use of their facilities. This work was supported, in part, by Grants-in-Aid for Cancer Research from the Ministry of Education, Culture, Science, Sports and Technology of Japan; in part by a Grant-in-Aid for the Third Comprehensive 10-Year Strategy for Cancer Control and for Cancer Research from the Ministry of Health, Labour and Welfare of Japan.

REFERENCES

1 Jemal A, Siegel R, Ward E *et al.* Cancer statistics, 2008. *CA Cancer J Clin* 2008; **58**: 71–96.
2 Gumbiner BM. Carcinogenesis: A balance between beta-catenin and APC. *Curr Biol* 1997; **7**: 443–6.
3 Kuwai T, Kitadai Y, Tanaka S *et al.* Single nucleotide polymorphism in the hypoxia-inducible factor-1alpha gene in colorectal carcinoma. *Oncol Rep* 2004; **12**: 1033–7.
4 Oue N, Kuniyasu H, Noguchi T *et al.* Serum concentration of Reg IV in patients with colorectal cancer: Overexpression and high serum levels of Reg IV are associated with liver metastasis. *Oncology* 2007; **72**: 371–80.
5 Tsukita S, Furuse M, Itoh M. Multifunctional strands in tight junctions. *Nat Rev Mol Cell Biol* 2001; **2**: 285–93.
6 Niimi T, Nagashima K, Ward JM *et al.* claudin-18, a novel downstream target gene for the T/EBP/NKX2.1 homeodomain transcription factor, encodes lung- and stomach-specific isoforms through alternative splicing. *Mol Cell Biol* 2001; **21**: 7380–90.
7 Sanada Y, Oue N, Mitani Y, Yoshida K, Nakayama H, Yasui W. Down-regulation of the claudin-18 gene, identified through serial analysis of gene expression data analysis, in gastric cancer with an intestinal phenotype. *J Pathol* 2006; **208**: 633–42.
8 Sahin U, Koslowski M, Dhaene K *et al.* Claudin-18 splice variant 2 is a pan-cancer target suitable for therapeutic antibody development. *Clin Cancer Res* 2008; **14**: 7624–34.
9 Zwiers A, Fuss IJ, Leijen S, Mulder CJ, Kraal G, Bouma G. Increased expression of the tight junction molecule claudin-18 A1 in both experimental colitis and ulcerative colitis. *Inflamm Bowel Dis* 2008; **14**: 1652–9.
10 Sentani K, Oue N, Tashiro T *et al.* Immunohistochemical staining of Reg IV and claudin-18 is useful in the diagnosis of gastrointestinal signet ring cell carcinoma. *Am J Surg Pathol* 2008; **32**: 1182–9.
11 Mees ST, Mennigen R, Spieker T *et al.* Expression of tight and adherens junction proteins in ulcerative colitis associated colorectal carcinoma: Upregulation of claudin-1, claudin-3, claudin-4, and beta-catenin. *Int J Colorectal Dis* 2009; **24**: 361–8.
12 Ueda J, Semba S, Chiba H *et al.* Heterogeneous expression of claudin-4 in human colorectal cancer: Decreased claudin-4 expression at the invasive front correlates cancer invasion and metastasis. *Pathobiology* 2007; **74**: 32–41.
13 Matsuda Y, Semba S, Ueda J *et al.* Gastric and intestinal claudin expression at the invasive front of gastric carcinoma. *Cancer Sci* 2007; **98**: 1014–9.
14 Kim YS, Gum J Jr, Brockhausen I. Mucin glycoproteins in neoplasia. *Glycoconj J* 1996; **13**: 693–707.
15 Tatematsu M, Ichinose M, Miki K, Hasegawa R, Kato T, Ito N. Gastric and intestinal phenotypic expression of human stomach cancers as revealed by pepsinogen immunohistochemistry and mucin histochemistry. *Acta Pathol Jpn* 1990; **40**: 494–504.
16 Yoshikawa A, Inada Ki K, Yamachika T, Shimizu N, Kaminishi M, Tatematsu M. Phenotypic shift in human differentiated gastric cancers from gastric to intestinal epithelial cell type during disease progression. *Gastric Cancer* 1998; **1**: 134–41.
17 Tajima Y, Yamazaki K, Nishino N *et al.* Gastric and intestinal phenotypic marker expression in gastric carcinomas and recurrence pattern after surgery-immunohistochemical analysis of 213 lesions. *Br J Cancer* 2004; **91**: 1342–8.
18 Hollingsworth MA, Swanson BJ. Mucins in cancer: Protection and control of the cell surface. *Nat Rev Cancer* 2004; **4**: 45–60.
19 Byrd JC, Bresalier RS. Mucins and mucin binding proteins in colorectal cancer. *Cancer Metastasis Rev* 2004; **23**: 77–99.
20 Eaden JA, Abrams KR, Mayberry JF. The risk of colorectal cancer in ulcerative colitis: A meta-analysis. *Gut* 2001; **48**: 526–35.
21 Tatsumi N, Kushima R, Vieth M *et al.* Cytokeratin 7/20 and mucin core protein expression in ulcerative colitis-associated colorectal neoplasms. *Virchows Arch* 2006; **448**: 756–62.
22 Femia AP, Tarquini E, Salvadori M *et al.* K-ras mutations and mucin profile in preneoplastic lesions and colon tumors induced in rats by 1,2-dimethylhydrazine. *Int J Cancer* 2008; **122**: 117–23.
23 Kocer B, McKolanis J, Soran A. Humoral immune response to MUC5AC in patients with colorectal polyps and colorectal carcinoma. *BMC Gastroenterol* 2006; **6**: 4.
24 Chawengsaksophak K, James R, Hammond VE, Kontgen F, Beck F. Homeosis and intestinal tumours in Cdx2 mutant mice. *Nature* 1997; **386**: 84–7.

25 Kaimaktchiev V, Terracciano L, Tornillo L *et al.* The homeobox intestinal differentiation factor CDX2 is selectively expressed in gastrointestinal adenocarcinomas. *Mod Pathol* 2004; **17**: 1392–9.

26 Hamilton SR, Aaltonen LA, eds. *World Health Organization Classification of Tumours. Pathology and Genetics of Tumours of the Digestive System.* Lyon: IARC Press, 2000.

27 Sobin LH, Wittekind CH, eds. *TNM Classification of Malignant Tumors*, 6th edn. New York: John Wiley & Sons, 2002; 65–8.

28 Mizoshita T, Tsukamoto T, Nakanishi H *et al.* Expression of Cdx2 and the phenotype of advanced gastric cancers: Relationship with prognosis. *J Cancer Res Clin Oncol* 2003; **129**: 727–34.

29 Oue N, Mitani Y, Aung PP *et al.* Expression and localization of Reg IV in human neoplastic and non-neoplastic tissues: Reg IV expression is associated with intestinal and neuroendocrine differentiation in gastric adenocarcinoma. *J Pathol* 2005; **207**: 185–98.

30 Mantel N. Evaluation of survival data and two new rank order statistics arising in its consideration. *Cancer Chemother Rep* 1966; **50**: 163–70.

31 Hough CD, Sherman-Baust CA, Pizer ES *et al.* Large-scale serial analysis of gene expression reveals genes differentially expressed in ovarian cancer. *Cancer Res* 2000; **60**: 6281–7.

32 Agarwal R, D'Souza T, Morin PJ. Claudin-3 and claudin-4 expression in ovarian epithelial cells enhances invasion and is associated with increased matrix metalloproteinase-2 activity. *Cancer Res* 2005; **65**: 7378–85.

33 Hoevel T, Macek R, Swisshelm K, Kubbies M. Reexpression of the TJ protein CLDN1 induces apoptosis in breast tumor spheroids. *Int J Cancer* 2004; **108**: 374–83.

34 Michl P, Barth C, Buchholz M *et al.* Claudin-4 expression decreases invasiveness and metastatic potential of pancreatic cancer. *Cancer Res* 2003; **63**: 6265–71.

35 Hewitt KJ, Agarwal R, Morin PJ. The claudin gene family: Expression in normal and neoplastic tissues. *BMC Cancer* 2006; **6**: 186.

36 Itzkowitz SH, Present DH. Consensus conference: Colorectal cancer screening and surveillance in inflammatory bowel disease. *Inflamm Bowel Dis* 2005; **11**: 314–21.

37 Yano K, Imaeda T, Niimi T. Transcriptional activation of the human claudin-18 gene promoter through two AP-1 motifs in PMA-stimulated MKN45 gastric cancer cells. *Am J Physiol Gastrointest Liver Physiol* 2008; **294**: 336–43.

38 Matsuda K, Yamauchi K, Matsumoto T, Sano K, Yamaoka Y, Ota H. Quantitative analysis of the effect of Helicobacter pylori on the expressions of SOX2, CDX2, MUC2, MUC5AC, MUC6, TFF1, TFF2, and TFF3 mRNAs in human gastric carcinoma cells. *Scand J Gastroenterol* 2008; **43**: 25–33.

39 Yao T, Tsutsumi S, Akaiwa Y *et al.* Phenotypic expression of colorectal adenocarcinomas with reference to tumor development and biological behavior. *Jpn J Cancer Res* 2001; **92**: 755–61.

40 Biemer-Huttmann AE, Walsh MD, McGuckin MA *et al.* Immunohistochemical staining patterns of MUC1, MUC2, MUC4, and MUC5AC mucins in hyperplastic polyps, serrated adenomas, and traditional adenomas of the colorectum. *J Histochem Cytochem* 1999; **47**: 1039–48.

41 Buisine MP, Janin A, Maunoury V *et al.* Aberrant expression of a human mucin gene (MUC5AC) in rectosigmoid villous adenoma. *Gastroenterology* 1996; **110**: 84–91.

42 Bartman AE, Sanderson SJ, Ewing SL *et al.* Aberrant expression of MUC5AC and MUC6 gastric mucin genes in colorectal polyps. *Int J Cancer* 1999; **80**: 210–18.

43 Myerscough N, Sylvester PA, Warren BF *et al.* Abnormal subcellular distribution of mature MUC2 and de novo MUC5AC mucins in adenomas of the rectum: Immunohistochemical detection using non-VNTR antibodies to MUC2 and MUC5AC peptide. *Glycoconj J* 2001; **18**: 907–14.

44 Mallo GV, Rechreche H, Frigerio JM *et al.* Molecular cloning, sequencing and expression of the mRNA encoding human Cdx1 and Cdx2 homeobox. Down-regulation of Cdx1 and Cdx2 mRNA expression during colorectal carcinogenesis. *Int J Cancer* 1997; **74**: 35–44.

45 Hinoi T, Tani M, Lucas PC *et al.* Loss of CDX2 expression and microsatellite instability are prominent features of large cell minimally differentiated carcinomas of the colon. *Am J Pathol* 2001; **159**: 2239–48.

46 Bonhomme C, Duluc I, Martin E *et al.* The Cdx2 homeobox gene has a tumour suppressor function in the distal colon in addition to a homeotic role during gut development. *Gut* 2003; **52**: 1465–71.

47 Hinoi T, Loda M, Fearon ER. Silencing of CDX2 expression in colon cancer via a dominant repression pathway. *J Biol Chem* 2003; **278**: 44608–16.

48 Satake S, Semba S, Matsuda Y *et al.* Cdx2 transcription factor regulates claudin-3 and claudin-4 expression during intestinal differentiation of gastric carcinoma. *Pathol Int* 2008; **58**: 156–63.

49 Park ET, Gum JR, Kakar S, Kwon SW, Deng G, Kim YS. Aberrant expression of SOX2 upregulates MUC5AC gastric foveolar mucin in mucinous cancers of the colorectum and related lesions. *Int J Cancer* 2008; **122**: 1253–60.

50 Tsukamoto T, Inada K, Tanaka H *et al.* Down-regulation of a gastric transcription factor, Sox2, and ectopic expression of intestinal homeobox genes, Cdx1 and Cdx2: Inverse correlation during progression from gastric/intestinal-mixed to complete intestinal metaplasia. *J Cancer Res Clin Oncol* 2004; **130**: 135–45.

51 Jass JR. Classification of colorectal cancer based on correlation of clinical, morphological and molecular features. *Histopathology* 2007; **50**: 113–30.

52 Hoos A, Urist MJ, Stojadinovic A *et al.* Validation of tissue microarrays for immunohistochemical profiling of cancer specimens using the example of human fibroblastic tumors. *Am J Pathol* 2001; **158**: 1245–51.

Pathology International 2010; **60**: 681–684 doi:10.1111/j.1440-1827.2010.02579.x

Case Report

Serous cystic neoplasm in an intrapancreatic accessory spleen

Shutaro Hori,[1] Satoshi Nara,[2] Kazuaki Shimada,[2] Hidenori Ojima,[1] Yae Kanai[1] and Nobuyoshi Hiraoka[1]

[1]Pathology Division, National Cancer Center Research Institute, and [2]Division of Hepato-Biliary and Pancreatic Surgery, National Cancer Center Hospital, Tokyo, Japan

Serous cystic neoplasm (SCN) of the pancreas is a benign epithelial neoplasm, except in extremely rare malignant cases. Development of SCN in tissues other than the pancreas has been never reported. Here we present the first reported case of SCN in an intrapancreatic accessory spleen (IPAS). A 54-year-old female patient with von Hippel-Lindau (VHL) syndrome was found to have pancreatic tail mass. Pathologically the 25-mm solid mass was an IPAS showing proliferation of clear cuboidal tumor cells without atypia, forming numerous small cysts. The tumor cells were rich in cytoplasmic glycogen and distributed in the splenic tissue almost diffusely. Immunohistochemically, tumor cells were positive for cytokeratins, MUC6, and neuron-specific enolase, and negative for neuroendocrine markers. From these findings, we diagnosed the lesion as SCN in IPAS. This tumor is suggested to develop as a VHL-associated SCN from coexisting pancreatic tissue in IPAS rather than as a metastatic tumor.

Key words: accessory spleen, pancreas, serous cystic neoplasm, von Hippel-Lindau syndrome

Serous cystic neoplasm (SCN) of the pancreas is a benign epithelial neoplasm that shows malignancy in only a handful of cases, and is composed of uniform cuboidal, glycogen-rich cells that mostly form numerous small cysts containing serous fluid.[1,2] Serous cystic neoplasm of the pancreas frequently occurs in pancreatic tissue as a solitary tumor, and no cases developing in tissues other than the pancreas have been reported. Serous cystic neoplasm can develop in association with von Hippel-Lindau (VHL) syndrome, which is an autosomal dominant neoplastic syndrome characterized by clear cell neoplasms including hemangioblastomas of the central nervous system, renal neoplasms, and clear cell endocrine pancreatic neoplasms.[1–3] Such cases of SCN associated with VHL syndrome are often multifocal.[1,2,4]

Intrapancreatic accessory spleen (IPAS) is seen in 2% of autopsy cases in the general population.[5] Development of epithelial neoplasm in accessory spleen is extremely rare, and all of the 25 tumors reported previously were epidermal cysts.[6–8] Here we present the first reported case of SCN in IPAS in a patient with VHL syndrome.

CLINICAL SUMMARY

A 54-year-old Japanese woman was admitted to our institution for a second opinion after several small tumors had been demonstrated in the pancreas by abdominal computed tomography (CT) at another hospital. She had undergone surgery for cerebellar and spinal hemangioblastoma at the ages of 37 and 38 years, respectively, and had been followed up for VHL syndrome for 16 years. Her mother and son had also been diagnosed as having VHL syndrome. On admission, she had no symptoms, and all clinical and laboratory data were normal. The serum levels of tumor markers (carcinoembryonic antigen and CA19-9) and pancreatic hormones (insulin and gastrin) were all within normal limits. Abdominal angiography revealed six hypervascular tumors in the pancreas: 3 in the head, 2 in the body, and 1 in the tail. Abdominal CT detected multiple small cysts throughout the pancreas in addition to these tumors, and neither renal nor adrenal tumors were evident. Our preoperative diagnosis was multiple endocrine tumors. The largest tumor, 32 mm in diameter, was located in the pancreas tail, and this was considered to have a high risk of malignancy. The other five tumors were less than 20 mm in diameter. We decided to resect the largest tumor by parenchyma-sparing enucleation. The operation was uneventful, and 6 months later, the patient was well without any tumor recurrence, metastasis, or progression of the five remaining pancreatic tumors.

Correspondence: Nobuyoshi Hiraoka, MD, PhD, Pathology Division, National Cancer Center Research Institute, 5-1-1 Tsukiji, Chuo-ku, Tokyo 104-0045, Japan. Email: nhiraoka@ncc.go.jp

Received 26 May 2010. Accepted for publication 1 June 2010.

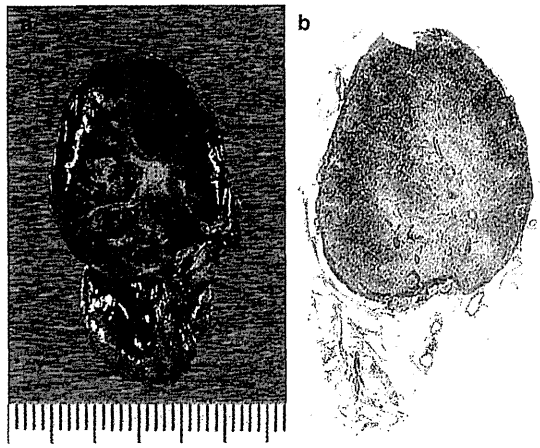

Figure 1 Freshly cut specimen of the mass in the pancreas tail (**a**), showing that it is encapsulated, with a reddish-tan solid appearance and a central stellate scar. Loupe view of the mass (**b**). The mass was located in an intrapancreatic accessory spleen showing proliferation of serous cystic neoplastic cells.

PATHOLOGICAL FINDINGS

Gross findings

An elastic-hard, solid, and spherical mass measuring 25 × 20 × 20 mm was present in the tail of the pancreas. At the cut surface, the well demarcated, reddish-tan solid mass was covered with a thin fibrous capsule (Fig. 1a). The mass was slightly elevated at the cut surface, and there was a central stellate scar in the tumor. A few microcystic lesions were evident in the pancreatic tissue.

Microscopic findings

Histologically, the mass was a completely encapsulated area of splenic tissue, i.e. IPAS, showing proliferation of clear

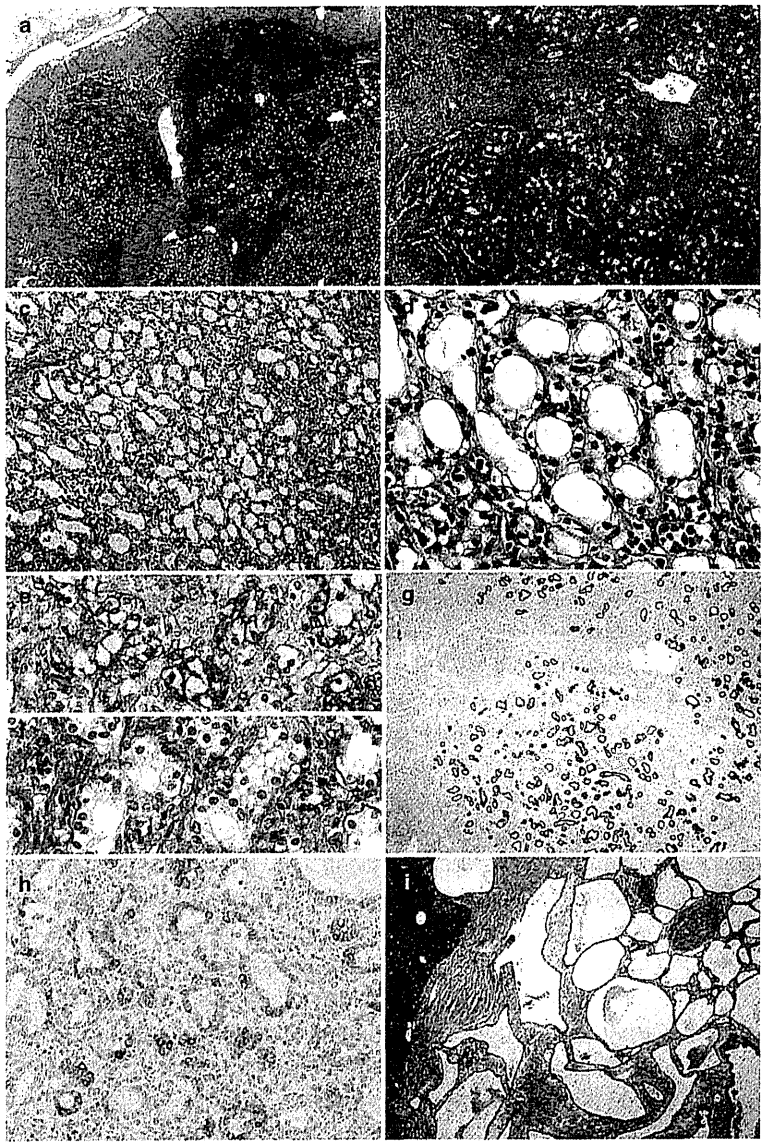

Figure 2 Histological features of the tumor (**a-d,i**). Splenic structures exhibiting a fibrous capsule, trabeculae, and red and white pulp, as revealed at very low (**a**) and low (**b**) power. The clear tumor cells form numerous small cysts in the splenic tissue sparsely (**a,b**) and densely (**c**). The nuclei of the tumor cells are small and round without atypia (**d**). Periodic acid-Schiff staining without (**e**) and with (**f**) diastase digestion highlights abundant glycogen in the tumor cells. Another serous cystic neoplasm is also present in the pancreatic parenchyma around the main mass (**i**). Immunohistochemical features of serous cystic neoplasm in the intrapancreatic accessory spleen (**g,h**). The tumor cells are strongly positive for cytokeratins (AE1/AE3) (**g**) and are also positive for MUC6 (**h**). Section shown in (**g**) is a serial section of that in (**b**).

Potential role for vascular endothelial growth factor-D as an autocrine factor for human gastric carcinoma cells

Miwako Tanaka,[1] Yasuhiko Kitadai,[1,4] Michiyo Kodama,[1] Kei Shinagawa,[1] Tomonori Sumida,[1] Shinji Tanaka,[2] Naohide Oue,[3] Wataru Yasui[3] and Kazuaki Chayama[1]

[1]Department of Medicine and Molecular Science, Hiroshima University Graduate School of Biomedical Sciences, Hiroshima; [2]Department of Endoscopy, Hiroshima University Hospital, Hiroshima; [3]Molecular Pathology, Hiroshima University Graduate School of Biomedical Sciences, Hiroshima, Japan

(Received April 5, 2010/Revised June 1, 2010/Accepted June 12, 2010/Accepted manuscript online June 17, 2010/Article first published online July 6, 2010)

Vascular endothelial growth factor (VEGF)-D induces lymphangiogenesis by activating VEGF receptor (VEGFR)-3, which is expressed mainly by lymphatic endothelial cells. VEGFR-3 has also been detected in several types of malignant cells, but the significance of VEGFR-3 expression by malignant cells remains unclear. We examined the expression and function of VEGF-D/VEGFR-3 in human gastric carcinoma cells. Expression of VEGF-D and VEGFR-3 was analyzed in three human gastric carcinoma cell lines and 29 surgical specimens. cDNA microarray analysis was used to examine the effect of VEGF-D on the expression of genes associated with disease progression in VEGFR-3-expressing KKLS cells. VEGF-D-transfected cells and control cells were transplanted into the gastric wall of nude mice. In 10 of the 29 (34%) gastric carcinoma specimens and two of the three cell lines, cancer cells expressed both VEGF-D and VEGFR-3. *In vitro* treatment of KKLS cells with exogenous VEGF-D increased expression of cyclin D1 and Bcl-2 and stimulated cell proliferation. VEGF-D transfection into KKLS cells resulted in stimulation of angiogenesis, lymphangiogenesis, and cell proliferation, and in inhibition of apoptosis. VEGF-D may participate in the progression of human gastric carcinoma by acting via autocrine and paracrine mechanisms. (*Cancer Sci* 2010; 101: 2121–2127)

Gastric cancer is one of the most frequently occurring malignancies in the world.[1] Acquisition of metastatic potential by tumor cells results in a poor prognosis for patients with gastric carcinoma. The extent of lymph node metastasis is one of the most important prognostic factors and determines the course of cancer therapy.[2]

Lymphangiogenesis and angiogenesis are regulated by members of the vascular endothelial growth factor (VEGF) family and their receptors.[3,4] VEGF-A is a major inducer of angiogenesis and vessel permeability.[5,6] The VEGF family includes VEGF-A, -B, -C, -D, -E, -F, and placental growth factor (PlGF).[7] VEGF-D, also known as c-fos-induced growth factor,[8] is secreted as a preprotein that undergoes proteolytic processing.[9] Full-length VEGF-D displays high affinity for VEGFR-3, whereas its affinity for VEGFR-2 is increased through progressive proteolytic cleavage.[9] In animal studies, VEGF-D has been shown to enhance tumor angiogenesis and lymphangiogenesis, thereby promoting metastatic spread of tumor cells via the lymphatics.[10–12] In clinical studies, correlation between expression of VEGF-D by tumor cells and lymph node metastasis has been reported.[13–18] In contrast, some clinical studies have shown that the level of VEGF-D expression is lower in tumor tissue than in the corresponding normal tissue.[19–23] Therefore, it remains controversial whether VEGF-D is the main regulator of lymphangiogenesis. Because of its structural similarity to VEGF-C, VEGF-D is thought to have a similar biologic effect. Recently, we studied the expression and role of the VEGF-C/VEGFR-3 axis in human gastric carcinoma.[24] We showed that the tumor cells expressed not only VEGF-C but also VEGFR-3. *In vitro and in vivo* experiments showed that VEGF-C acts as a progressive growth factor, in addition to acting as a lymphangiogenic and angiogenic factor. However, the autocrine role of VEGF-D in gastric carcinoma cells has not been characterized. Thus, we analyzed the role of the VEGF-D/VEGFR-3 axis in human gastric carcinoma cells.

Materials and Methods

Surgical specimens of gastric carcinoma. Paraffin-embedded archival specimens of invasive gastric carcinoma obtained from 29 patients who underwent surgical resection at Hiroshima University Hospital were studied by immunohistochemistry. All tumors had invaded beyond the submucosa. The criteria for staging and histologic classification were those proposed by the Japanese Research Society for Gastric Cancer.[25] The patient group comprised 27 men and two women, with a median age of 66 years (range, 34–81 years). The tissues were immediately snap-frozen and stored in liquid nitrogen for semiquantitative RT-PCR.

Cell cultures. Three cell lines established from human gastric carcinomas were maintained in RPMI-1640 medium (Nissui, Tokyo, Japan) with 10% FBS (MA BioProducts, Walkersville, MD, USA). The TMK-1 cell line (derived from poorly differentiated adenocarcinoma) was provided by Dr E. Tahara (Hiroshima University, Hiroshima, Japan). The KKLS cell line (derived from undifferentiated carcinoma) was provided by Dr Y. Takahashi (Chiba University, Chiba, Japan). The MKN-1 cell line (derived from adenosquamous carcinoma) was obtained from the Health Science Research Resources Bank (Osaka, Japan).

Cell proliferation assay. *In vitro* growth was measured with a Cell Proliferation Biotrak ELISA System, version 2 (Amersham Biosciences, Piscataway, NJ, USA) according to the manufacturer's instructions to determine whether recombinant human VEGF-D (rhVEGF-D) (R&D Systems, Minneapolis, MN, USA) would stimulate proliferation of KKLS cells and TMK-1 cells. Cells (1×10^4) were seeded on a 96-well plate, and BrdU (final concentration, 10 μM) was added to the culture medium with or without rhVEGF-D (2, 20, or 100 ng/mL) for 24 h. Cell proliferation was quantified in a plate reader (Microplate Manager 5.2.1; Bio-Rad, Hercules, CA, USA) at 450 nm.

[4]To whom correspondence should be addressed.
E-mail: kitadai@hiroshima-u.ac.jp

doi: 10.1111/j.1349-7006.2010.01649.x

Microarray analysis. We performed microarray analysis using the Human Cancer CHIP (version 4; Takara Shuzo, Kyoto, Japan), in which 886 human cancer-related genes are spotted on glass plates. KKLS cells were cultured in RPMI-1640 medium without FBS for 6 h and then cultured with or without rhVEGF-D (20 ng/mL) for 8 h. A fluorescent probe synthesized by reverse transcription of 1 μg of the mRNA with 50 U AMV reverse transcriptase (Takara Shuzo) was added to each reaction mixture. Cy3- and Cy5-labeled probes were prepared by using mRNAs isolated from control cells and rhVEGF-D cells, and both were mixed in the reaction buffer (6× SSC/0.2% SDS and 5× Denhardt's solution, 0.8 mg/mL poly [dA], and 1 mg/mL yeast tRNA). The mixture was hybridized to the cDNA CHIP at 65°C overnight. The CHIP was washed twice with 2× SSC/0.2% SDS solution at 55°C for 30 min and then with the same solution at 65°C for 5 min. Finally, the CHIP was washed with 0.05 × SSC at room temperature for 10 min. Signals on the hybridized CHIP were visualized and quantified with a ScanArray 5000 laser scanner (GSI Lomonids) and normalized to the averaged signals of housekeeping genes. Genes were excluded from further investigation when the intensities of both Cy3 and Cy5 were below 1000 fluorescence units. Those with Cy3/Cy5 signal ratios >2.0 were regarded as up-regulated.

Semiquantitative reverse transcription-polymerase chain reaction (RT-PCR) and quantitative real-time PCR. Total RNA was extracted from the gastric cancer cell lines with an RNeasy Kit (Qiagen, Tokyo, Japan) according to the manufacturer's instructions. RT-PCR was performed with the isolated RNA (1 μg). cDNA was generated from 1 μg of total RNA with a First-Strand cDNA Synthesis Kit (Amersham Biosciences, Buckinghamshire, UK). The primers and annealing temperatures for VEGF-D, VEGFR-2, VEGFR-3, β-actin, GAPDH, and Bcl-2 are given in Table 1. The primers were designed with specific Primer analysis software (Primer Designer; Scientific and Educational Software, Arlington, MA, USA), and the specificities of the sequences were confirmed by FASTA analysis (EMBL Nucleotide Sequence Database). Semiquantitative RT-PCR was performed with an AmpliTaq Gold Kit (Roche, Mannheim, Germany), and quantitative real-time PCR was performed with a LightCycler-FastStart DNA Master SYBR-Green I Kit (Roche) according to the manufacturer's instructions. Quantitative real-time PCR was used to monitor gene expression and was performed with a LightCycler system and Light Cycler Data Analysis Software version 3.5 (Roche) according to standard procedures. To correct for differences in both RNA quality and quantity between samples, the data were normalized to those for β-actin.

Immunofluorescence staining for pVEGFR-3. KKLS cells were cultured in RPMI-1640 medium without FBS for 24 h, then treated with or without rhVEGF-D (20 ng/mL) for 10 min. pVEGFR-2,3 (1:1000; Calbiochem, San Diego, CA, USA) was used to stain pVEGFR-2,3 in tumor cells.

Western blot analysis. Western blotting was used to evaluate the expression of cyclin D1, Akt and MAPK, p38, and JNK phosphorylation. To evaluate Akt, MAPK, p38, and JNK phosphorylation of KKLS cells, cells were plated at 1.5×10^5 cells/mL per well in a six-well plate and incubated overnight. Cells were then starved for 24 h in serum-free medium and stimulated with rhVEGF-D (20 ng/mL) or rhVEGF-C (20 ng/mL) (R&D Systems) for 10 min at 37°C. After stimulation, cells were washed three times in cold PBS containing 1 mmol/L sodium. Cell lysates were prepared with M-PER Mammalian Protein Extraction Reagent (Pierce, Rockford, IL, USA). Samples of cell lysates (20 μg protein) were separated by SDS-PAGE and transferred to nitrocellulose transfer membranes (Whatman, Dassel, Germany). Blots were blocked for 1 h at room temperature in TBS containing 1% skim milk and 0.1% Tween 20. Membranes were incubated overnight at 4°C with primary antibodies against polyclonal mouse antihuman cyclin D1 (Dako, Glostrup, Denmark), polyclonal rabbit antibody to phospho-Akt (phosphorylated at Ser473; Cell Signaling Technology, Beverly, MA, USA), phospho-MAPK, p38, JNK (Promega, Madison, WI, USA), and β-actin (Sigma, St. Louis, MO, USA). Membranes were then washed three times in TBS containing 0.1% Tween 20 and incubated with secondary antibody for 1 h at room temperature. Immune complexes were visualized by enhanced chemiluminescence with an ECL Plus Kit (Amersham Biosciences).

Gene transfection and cloning of transfected cell lines. Full-length human VEGF-D cDNA was inserted into the EcoRI-EcoRI site of pBR322 (Invitrogen, Carlsbad, CA, USA). The resultant plasmid was digested with XbaI-BamHI and cloned into the XbaI-BamHI site of the pcDNA4/myc-His vector (Invitrogen) to yield VEGF-D expression. Expression of VEGF-D cDNA was under the control of the cytomegalovirus promoter. KKLS cells were transfected with either the full-length VEGF-D cDNA or empty pcDNA4/myc-His vector by using Lipofectin (Life Technologies, Gaithersburg, MD, USA) according to the manufacturer's instructions. After transfection, cells were grown in selective medium (10% FBS-RPMI-1640 containing 400 μg/mL Zeocin). Zeocin-resistant colonies were lifted from culture dishes and grown individually to establish stable VEGF-D-overexpressing clonal lines.

Enzyme-linked immunosorbent assay (ELISA) for VEGF-D protein. KKLS cells were plated at 1.5×10^5 cells/mL per well

Table 1. Application of PCR

Gene	Primer sequences	Number of cycles	Annealing temperature	Product size (bp)
VEGF-D	F: 5′-GTATGGACTCTCGCTCAGCAT-3′ R: 5′-AGGCTCTCTTCATTGCAACAG-3′	32	59	226
VEGFR-2	F: 5′-GCATCTCATCTGTTACAGC-3′ R: 5′-CTTCATCAATCTTTACCCC-3′	32	62	331
VEGFR-3	F: 5′-GGTTCCTCCAGGATGAAGAC-3′ R: 5′-CAAGCAGTAACGCCAGTGTC-3′	32	62	505
β-Actin	F: 5′-GGACTTCGAGCAAGAGATGG-3′ R: 5′-AGCACTGTGTTGGCGTACAG-3′	35	55	234
GAPDH	F: 5′-ATCATCCCTGCCTCTACTGG-3′ R: 5′-CCCTCCGACGCCTGCTTCAC-3′	28	55	188
Bcl-2	F: 5′-GGTGGAGGAGCTCTTCCAGG-3′ R: 5′-ACAGTTCCACAAAGGCATCC-3′	35	60	206

VEGF-D, vascular endothelial growth factor D; VEGFR-2, VEGF receptor 2.

doi: 10.1111/j.1349-7006.2010.01649.x

in a six-well plate (Becton Dickinson Labware, Franklin Lakes, NJ, USA) and cultured in RPMI-1640 containing 10% FBS. After 48 h, the supernatants were collected and used to measure VEGF-D protein. We used the Quantikine Human VEGF-D Immunoassay (R&D Systems) according to the manufacturer's instructions to measure VEGF-D levels.

***In vitro* cell growth.** Cells (1×10^4) were seeded in a six-well plate and cultured in RPMI-1640 containing 0.5% FBS. The medium was changed every 48 h. Cell counts were determined with a Countess Automated Cell Counter (Invitrogen) from triplicate cultures.

Animal models. Male athymic BALB/c nude mice were obtained from Charles River Japan (Tokyo, Japan). The mice were maintained under specific pathogen-free conditions and used when 5 weeks old. Experiments were done according to the animal experimental guidelines of Hiroshima University.

Orthotopic (gastric mucosa) xenograft model. To produce gastric tumors, KKLS/VEGF-D and KKLS/control cells growing in culture were harvested from subconfluent cultures by brief treatment with 0.25% trypsin and 0.02% EDTA. Cells (1×10^6) were resuspended in HANKS and implanted into the gastric wall of nude mice under a zoom stereo microscope. After 4 weeks, the mice were killed and tumors were resected for study.

Immunohistochemistry. Formalin-fixed, paraffin-embedded serial sections (4 μm) were deparaffinized and rehydrated. Sections were immunostained for VEGF-D, VEGFR-3, Ki-67, and Lyve1. Antigen retrieval was performed in Dako REAL Target Retrieval Solution (Dako) in a microwave oven for 10 min. Endogenous peroxidase activity was blocked with 3% hydrogen peroxide in 100% methanol for 10 min. Sections were washed with PBS and blocked with 3% normal horse serum for 10 min. Frozen sections (8 μm) were immunostained for CD31 and fixed in cold acetone for 10 min. VEGF-D was detected with goat antihuman polyclonal antibody (1:200; R&D Systems), and VEGFR-3 was detected with goat antihuman polyclonal antibody (1:50; R&D Systems). Ki-67 was detected with mouse antihuman polyclonal antibody (MIB-1, 1:25; Dako), and Lyve1 was detected with rat antimouse monoclonal antibody (1:20; R&D Systems). CD31 was detected with rat antimouse polyclonal antibody (1:200; Pharmingen, San Diego, CA, USA). Sections were incubated overnight at 4°C with the primary antibodies. Sections were then washed with PBS three times and incubated for 1 h with peroxidase-conjugated secondary antibody. A positive reaction was detected by exposure to stable 3,3′-diaminobenzidine. The slides were counterstained with hematoxylin.

Quantification of Ki-67 labeling index, lymphatic vessel density (LVD), and Microvessel density (MVD). MVD was determined from the counts of CD31-positive vessels. Vessel density was assessed by light microscopy of the intratumoral and peritumoral lesions containing the greatest number of capillaries and small venules. Highly vascular areas were identified by scanning tumor sections at low power (×40 and ×100). After the six areas of greatest neovascularization were identified, a vessel count was performed at ×400, and the mean count of six fields was calculated and defined as the mean MVD. Identification of a vessel lumen was not necessary for a structure to be defined as a vessel.[26] Lymphatic activity was evaluated according to the area of lymphatic vessels stained with anti-Lyve1 antibody. For quantification of the lymphatic vessel area, six random fields at ×400 magnification were captured for each tumor, and the outline of each lymphatic vessel including a lumen was manually traced. The area was then calculated with the use of NIH ImageJ software. Ki-67 staining was assessed by determining the Ki-67 labeling index by means of light microscopy at the sites of the greatest number of Ki-67-positive cells. Cells were counted in ten fields at ×40 magnification, and the mean percentage of stained cells was calculated. The mean percentage of Ki-67-positive cells was taken as the Ki-67 labeling index.

Histochemical detection of apoptosis and determination of apoptotic index. Apoptotic cells in tissue sections were detected by terminal deoxynucleotide transferase-mediated TUNEL with the ApopTag Plus Peroxidase *In Situ* Apoptosis Detection Kit (Chemicon, Temecula, CA, USA) according to manufacturer's instructions. The apoptotic index was expressed as the ratio of positively stained tumor cells and bodies to all tumor cells, given as a percentage for each case. Five random fields in a section were selected by light microscopy; at least 1000 cells were counted under ×400 magnification.

Statistical analysis. The chi-squared test was used for analysis of categoric data, and the Mann–Whitney *U*-test was used for analysis of continuous variables. The significance level was set at 5% for all analysis.

Results

Immunohistochemistry for VEGF-D and VEGFR-3 in human gastric carcinoma tissues. We examined expression of VEGF-D and VEGFR-3 protein in 29 human gastric carcinoma tissues by immunohistochemistry. VEGFR-3 expression was observed on lymphatic endothelial cells. Of the 29 specimens of gastric carcinoma, 14 (48%) showed intense VEGF-D immunoreactivity (Fig. 1a,b), and 15 (52%) showed intense VEGFR-3 immunoreactivity (Fig. 1c,d) on tumor cells. In 10 of the 29 (34%) gastric carcinoma specimens, tumor cells expressed both VEGF-D and VEGFR-3. When the VEGF-D expression was analyzed in relation to histological types, positivity for VEGF-D in the diffuse (undifferentiated) type (7/10, 70%) was significantly higher than that in the intestinal (differentiated) type (7/19, 36%).

Expression of VEGF-D, VEGFR-2, VEGFR-3 mRNA in gastric carcinoma cell lines. We examined expression of VEGF-D, VEGFR-2, VEGFR-3 mRNA in gastric cancer cell lines by semiquantitative RT-PCR. All gastric carcinoma cell lines constitutively expressed VEGF-D mRNA. Expression of VEGFR-2 mRNA was not observed in any of the cell lines examined. Two of the three cell lines expressed VEGFR-3 mRNA (Fig. 2a). KKLS cells expressed VEGFR-3 at a high level; therefore, we used KKLS cells for further studies. Treatment of KKLS cells with VEGF-D induced phosphorylation of VEGFR-3 (Fig. 1e,f) and its downstream signaling molecule, Akt (Fig. 2b). Furthermore, treatment of KKLS cells with VEGF-D resulted in stimulation of cell proliferation. Treatment with VEGF-D did not stimulate proliferation of TMK-1 cells (VEGFR-3 negative) (Fig. 2c).

VEGF-D up-regulated expression of several genes associated with disease progression in KKLS cells. To investigate the various cancer-related genes up-regulated by VEGF-D, we performed microarray analysis. Various mRNA expression levels were compared between control KKLS cells and cells treated with rhVEGF-D for 8 h. Microarray analysis revealed up-regulation of 52 genes by VEGF-D stimulation. Representative genes that were up-regulated in cells treated with rhVEGF-D are shown in Table 2. Among these genes, we confirmed increased expression of Bcl-2 by quantitative real-time PCR (Fig. 3a) and of cyclin D1 (Fig. 3b) by western blotting. Treatment with VEGF-D increased expression of Bcl-2 mRNA and cyclin D1 protein.

Establishment of VEGF-D-overexpressing clonal cell line. To examine the biological function of VEGF-D, VEGF-D expression vector or the empty vector was stably transfected into KKLS cells. Overexpression of VEGF-D mRNA and protein was confirmed by quantitative real-time PCR (Fig. 4a) and ELISA (Fig. 4b), respectively.

***In vitro* and *in vivo* proliferation of VEGF-D-transfected KKLS cells.** The effect of overexpression of VEGF-D on the ability of